DOI: 10.1002/ejic.201001176

Synthesis and Structural Characterization of a Series of New Chiral-at-Metal Ruthenium Allenylidene Complexes

Stephen Costin,[a] Andria K. Widaman,[a] Nigam P. Rath,[a,b] and Eike B. Bauer*[a]

Keywords: P ligands / Ruthenium / Chirality

New chiral-at-metal ruthenium indenyl PPh_3 phosphoramidite allenylidene complexes have been synthesized and structurally characterized. Through thermal ligand-exchange reactions with $[RuCl(Ind)(PPh_3)_2]$, the phosphoramidite ligands (*R*)-binol-*N*,*N*-dimethylphosphoramidite (**5a**), (*R*)-binol-*N*,*N*-dibenzylphosphoramidite (**5b**), (*R*,*S*)-binol-*N*-benzyl-*N*-α-methylbenzylphosphoramidite (**5c**), and (*R*)-catechol-2-methylpyrrolidinephosphoramidite [(*R*)-**10**] were converted into the complexes $[RuCl(Ind)(PPh_3)(L)]$ [L = **5a**, 79 %; **5b**, 87 %; **5c**, 80 %, (*R*)-**10**, 67 %]. The complexes $[RuCl(Ind)(PPh_3)(\mathbf{5b})]$ and $[RuCl(Ind)(PPh_3)(\mathbf{5c})]$ were obtained diastereomerically pure and, by reaction with propargylic alcohols, subsequently converted into the allenylidene complexes $[Ru(Ind)(PPh_3)(\mathbf{5b})(=C=C=CRR')]^+PF_6^-$ (R = R′ = Ph, 85 %; R = Ph, R′ = Me, 66 %; R = 2-furyl, R′ = Me, 94 %; R = R′ = 4-fluorophenyl, 76 %; R = 4-methoxyphenyl, R′ = Me, 66 %) and $[Ru(Ind)(PPh_3)(\mathbf{5c})(=C=C=CRR')]^+PF_6^-$ (R = R′ = Ph, 91 %; R = Ph, R′ = Me, 72 %; R = 2-furyl, R′ = Me, 93 %), which were also obtained diastereomerically pure. Complex $[RuCl(Ind)(PPh_3)(\mathbf{5b})]$ and three of the new allenylidene complexes were characterized structurally, which showed that the chiral information was transferred from the precursor complex to the corresponding allenylidenes. Dynamic NMR experiments showed that during the synthesis of allenylidene complexes only one diastereomer was formed. The research presented herein has an impact on the chemistry of chiral allenylidene complexes as catalysts and as potential intermediates in propargylic substitution reactions.

Introduction

Allenylidene complexes are cumulene-type organometallic architectures of the general formula $[L_nM=C=C=CRR']$.[1] Although known since the 1970s,[2] their systematic investigation was significantly advanced when Selegue found in 1982 that allenylidene complexes **2** are readily accessible from propargylic alcohols **1** and an appropriate precursor complex in the presence of MPF_6 (Scheme 1).[3] Since then, a variety of allenylidene complexes have been synthesized and characterized. The majority of allenylidene complexes are based on ruthenium,[4] but other metals have been used as well, for example, Cr and W,[5a] Mo,[5b] Mn,[2b] Re,[5c] Ir,[5d] Rh,[1f] Fe,[5e] Os,[5f,5g] Pd,[5h,5i] and Ni.[6]

Allenylidenes play an important dual role as catalysts and intermediates in a number of catalytic transformations.[7] Some ruthenium allenylidene complexes are efficient catalyst precursors in ring-closing metathesis reactions,[8a–8d] ring-opening metathesis polymerization,[8e,8f] and in the dehydrogenative dimerization of tin hydrides.[9] Calculations[10] as well as reactivity studies[11] have shown that the C_α and C_γ atoms of the allenylidene chain are electrophilic,

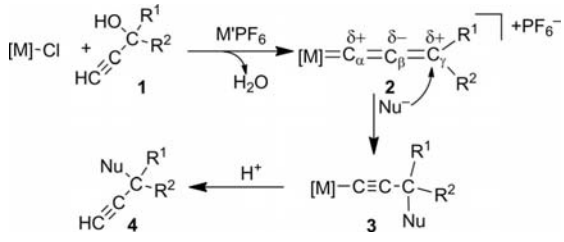

Scheme 1. Allenylidene complex formation and reactivity.

whereas the C_β atom is nucleophilic. Thus, the C_β atom can be protonated[11a] and the C_α and C_γ atoms react with nucleophiles. Attack of the C_γ atom by monofunctional nucleophiles leads to the alkynyl complex **3** (Scheme 1), which delivers the substituted product **4** after protonolysis.[12] Thus, the whole sequence in Scheme 1 represents a propargylic substitution reaction via an allenylidene intermediate.[12] Nicholas described a multistep sequence for such propargylic substitution reactions employing stoichiometric amounts of toxic $[Co_2(CO)_8]$ and involving cobalt-stabilized propargylic cations as intermediates.[13] Stoichiometric multistep alternatives following the path depicted in Scheme 1 have been described in the literature.[4g] Dimeric[14] and monomeric[15] ruthenium complexes have been shown to catalyze propargylic substitution reactions with a variety of carbon and heteroatom nucleophiles, for which allenylidene complexes were suggested as intermediates. Chiral ruthenium dimeric complexes $[RuCl(Cp^*)(\mu\text{-}S^*R)]_2$

[a] Department of Chemistry and Biochemistry, University of Missouri – St. Louis,
1, University Boulevard, St. Louis, MO 63121, USA
E-mail: bauere@umsl.edu
[b] Center for Nanoscience, University of Missouri – St. Louis,
1, University Boulevard, St. Louis, MO 63121, USA
Supporting information for this article is available on the WWW under http://dx.doi.org/10.1002/ejic.201001176.

(S*R = chiral thiolate) catalyze enantioselective substitution and cyclization reactions with enantiomeric excesses between 68 and 99%.[16]

Chiral allenylidene complexes have been far less investigated than their achiral counterparts. In addition to the dimeric chiral thiolate ruthenium complexes mentioned above, a chiral (*R*)-binap ruthenium indenyl allenylidene complex has been used in a multistep procedure (similar to Scheme 1) to synthesize optically active γ-keto alkynes.[17a] In a related procedure, Gimeno and co-workers took advantage of the chiral allenylidenes derived from chiral propargylic alcohols to prepare optically active alkynes by reaction with different nucleophiles.[4g,17b,17c] Aromatic π–π interactions in optically active ruthenium allenylidene complexes have been reported to play an important role in stereoselection in potential catalytic substitution reactions involving allenylidene intermediates.[17d]

Chiral-at-metal allenylidene complexes are rare. We are aware of only two examples in the literature to date. Gimeno and co-workers synthesized a chiral-at-metal ruthenium indenyl complex with an optically active diphenylphosphane ferrocenyl oxazoline ligand, which was converted into the corresponding allenylidene complex.[18a] Similarly, Matsuo and co-workers synthesized and structurally characterized a chiral-at-metal ruthenium fullerene cyclopentadienyl allenylidene complex with the chiral chelate ligand 1,2-bis(diphenylphosphanyl)propane.[18b] In both cases, the allenylidene complexes exhibit stereogenic centers at both the metal and ligand, and were obtained with diastereomeric purity. Some chiral-at-metal allenylidene complexes synthesized from achiral starting materials are known and have been isolated as racemic mixtures.[4k,4m]

We are interested in chiral-at-metal complexes[19] as it has been shown that some of them are promising catalysts for producing high enantiomeric excesses in a number of enantioselective organic transformations.[20] We therefore set out to advance the chemistry of chiral-at-metal allenylidene complexes and began to search for a general systematic approach to this class of compound. The starting points of our investigations were chiral-at-metal ruthenium chloro phosphoramidite complexes. Phosphoramidites (**5** in Figure 1) are a class of versatile monodendate ligands[21] that are easy to synthesize and they have been increasingly used as ligands in transition-metal-catalyzed organic transformations.[22] We have already synthesized the chiral-at-metal ruthenium chloro cyclopentadienyl complex **6** (Figure 1) as a single optically pure diastereomer and employed it as a catalyst in the Mukaiyama aldol reaction.[23]

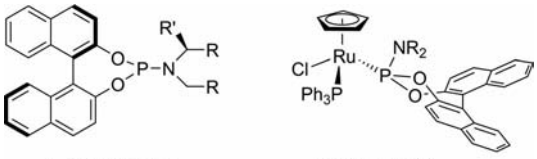

5 R = R' = H, **a**
R = Ph, R' = H, **b**
R = Ph, R' = CH_3, **c**

6 R = CH_2Ph

Figure 1. Phosphoramidites and a ruthenium complex thereof.

Complex **6** could be converted into the corresponding allenylidene complex but analytically pure material could not be isolated. We thus started to investigate structurally related indenyl alternatives. Indenyl complexes show increased reactivity in ligand-exchange reactions[24] and as catalysts,[25] referred to in the literature as the "indenyl effect".[26]

Herein, we describe a general, convenient, high-yielding route to optically pure chiral-at-metal allenylidene indenyl ruthenium complexes. These allenylidene complexes were obtained from the corresponding chiral-at-metal ruthenium chloro complexes with chirality transfer and are the first examples of allenylidene complexes with phosphoramidite ligands. A portion of this work has been communicated previously.[27]

Results

Ligand and Precursor Complex Syntheses

The majority of previously reported phosphoramidite ligands were derived from binol (see Figure 1). We were first interested in determining whether a simpler and thus cheaper diol could be employed in ligand and metal complex synthesis. By employing standard literature procedures,[21] catechol (**7**) was converted into the chiral phosphoramidite (*R*)-**10** by using the commercial (*R*)-2-methylpyrrolidine (**9**) as the amine (Scheme 2). In a two-step, one-pot procedure, the catechol was first converted into the corresponding phosphorochloridite **8**, which was further processed to the phosphoramidite (*R*)-**10**. The new ligand was obtained as a yellow oil in 78% isolated yield after purification by filtration and extraction.

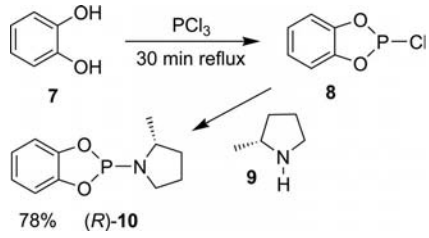

Scheme 2. Phosphoramidite synthesis.

Our previously synthesized chiral-at-metal ruthenium cyclopentadienyl phosphoramidite complex **6** (Figure 1) was obtained from the precursor complex [RuCl(Cp)(PPh_3)$_2$] by thermal PPh_3 exchange.[23] To obtain the corresponding indenyl ruthenium complexes, we envisaged a similar ligand exchange using the known[28] ruthenium complex [RuCl(Ind)(PPh_3)$_2$] (**11**, Ind = indenyl), which has previously been successfully employed in similar ligand-exchange reactions.[26e] Accordingly, the phosphoramidite ligands **5a**–**c** and (*R*)-**10** were heated with **11** in toluene or THF for 1–3 hours (Scheme 3). Chromatographic work-up afforded the corresponding ruthenium complexes **12a**–**d** as red-orange powders in 67–87% isolated yields. The employment of toluene in the synthesis of **12a** and **12d** was necessary as we

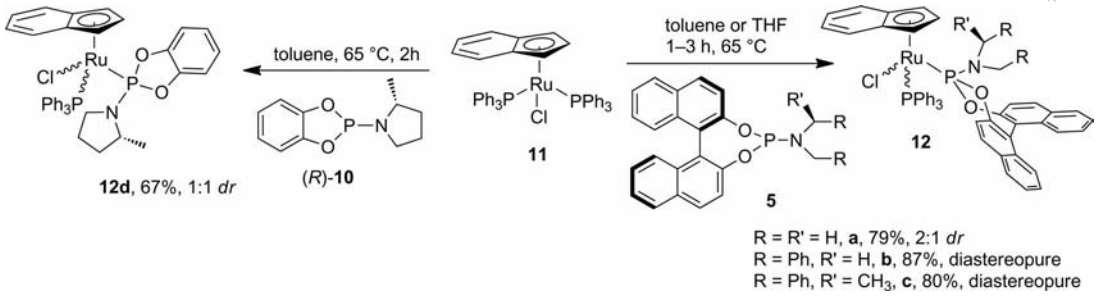

Scheme 3. Synthesis of chiral-at-metal chloro phosphoramidite complexes **12**.

could not remove THF, even by column chromatography. The new complexes are chiral at the metal and have been characterized by NMR (^{1}H, ^{13}C, ^{31}P), MS, IR, and, in most cases, by elemental analysis.

The coordination of one phosphoramidite and one PPh_3 ligand is readily indicated by two distinct ^{31}P NMR signals, which exhibit $^2J_{PP}$ couplings between 58.5 and 77.0 Hz, as expected for complexes with two different phosphorus atoms in a metal coordination sphere. As deduced from the NMR spectroscopic data, complexes **12a** and **12d** were isolated as a mixture of diastereomers, whereas complexes **12b** and **12c** were obtained as single optically pure diastereomers. The ^{31}P NMR spectra of **12a** and **12d** showed two sets of signals, and some signals in the ^{1}H NMR were doubled, revealing a diastereomeric ratio (*dr*) of 2:1 for **12a** and 1:1 for **12d**. We speculate that the smaller phosphoramidite ligands in **12a** and **12d** create only slight steric congestion at the metal, rendering the two diastereomers close in energy. For complexes **12b** and **12c** bearing larger phosphoramidite ligands, only one set of NMR signals was observed in the crude material as well as after purification, which suggests that only one diastereomer was formed. The indenyl ligand gives very distinct ^{1}H and ^{13}C NMR signals for the three protons and five carbon atoms of its coordinated five-membered ring.[26e] As a result of the stereogenic centers at the metal and ligand, all these carbons and protons are diastereotopic and give individual signals in the corresponding NMR spectra.

To unequivocally establish the structures of the new ruthenium complexes, the X-ray structure of complex **12b** was determined (Tables 1 and 2, Figure 2). The structure closely resembles that of the cyclopentadienyl analogue **6** (Figure 1), which was structurally characterized previously.[23] To obtain information about the impact of the coordination of phosphoramidite ligands on their structures, an X-ray determination of the ligand **5b** was also performed (Tables 1

Table 1. Selected bond lengths and angles.

Bond lengths [Å][a]	**5b**	**12b**·(CH_2Cl_2)	[**15a**][PF_6]·(CH_2Cl_2)	[**15b**][PF_6]·(CH_2Cl_2)$_2$	[**15d**][PF_6]	**13**
Ru1–P1	–	2.1961(7)	2.2730(6)	2.2729(5)	2.2680(8)	2.321(2)
Ru1–P2	–	2.3504(8)	2.3131(7)	2.3037(5)	2.3217(9)	2.358(2)
Ru1–Cl1	–	2.4439(7)	–	–	–	–
Ru1–C10	–	–	1.887(2)	1.8937(19)	1.870(4)	1.878(5)
C10–C11	–	–	1.250(4)	1.250(3)	1.256(6)	1.260(7)
C11–C12	–	–	1.357(4)	1.348(3)	1.346(7)	1.353(7)
P1–N1	1.648(3)	1.663(3)	1.644(2)	1.6467(17)	1.654(3)	–
Bond angles [°]						
C10–Ru1–P1	–	89.28(3)[b]	92.73(7)	92.39(6)	89.59(11)	88.7(2)
C10–Ru1–P2	–	86.99(3)[b]	85.82(7)	84.81(6)	85.31(13)	97.4(2)
P1–Ru1–P2	–	98.87(3)	100.13(2)	100.416(17)	100.12(3)	96.95(5)
C10–C11–C12	–	–	177.6(3)	174.9(2)	174.8(5)	168.2(7)
C11–C12–C*X*	–		120.1(3) (*X* = 13)	120.76(19) (*X* = 14)	124.8(8) (*X* = 10)	118.2(6)
O1–P1–O2	97.37(10)	99.58(10)	100.12(9)	99.76(7)	100.46(13)	–
O1–P1–N1	108.90(12)	108.61(12)	110.33(11)	96.36(8)	96.61(16)	–
O2–P1–N1	96.48(11)	95.13(12)	95.56(10)	109.91(8)	109.05(14)	–
Other geometrical parameters						
Ru–Cp [Å][c]	–	1.909	1.927	1.931	1.940	1.951(5)
Dihedral angle [°][d]	–	–	34.4	14.8	27.6	15.5(3)
Deviation from planarity at nitrogen [Å][e]	0.0305	0.0281	0.0108	0.0104	0.0045	–

[a] C10–C11–C12 is C1–C2–C3 in complex **15d**. [b] Cl1–Ru1–P1 and Cl1–Ru1–P2, respectively. [c] Distance between the centroid of Cp of the indenyl ligand and the ruthenium center. [d] Angle between the planes defined by the Cp centroid, Ru, C10 and C10–C11–C12–C13 (**15a**,**b**) and C1–C2–C3–C4 (**15d**), respectively. [e] Average deviation from a least-squares mean plane defined by N1, P1 and C21, C28 (**5b**), C30, C37 (**12b**), C25, C32 (**15a**), C38, C45 (**15b**), and C45, C52 (**15d**) [see Equation (1)].

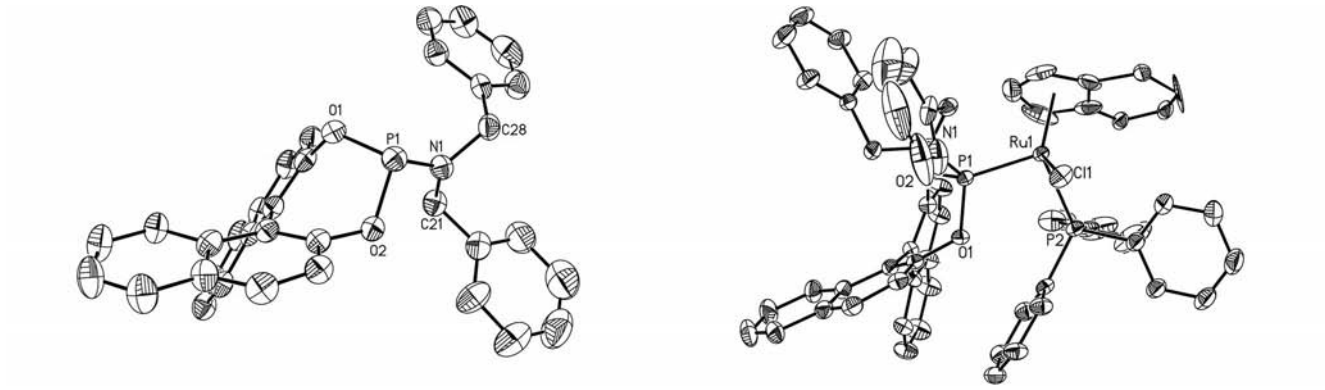

Figure 2. Molecular structures of **5b** (left) and **12b** (right). Ellipsoids are shown at the 30% probability level. Hydrogen atoms and solvent molecules have been omitted for clarity. For key bond lengths and bond angles, see Table 1.

and 2, Figure 2). The structure features a planar geometry at the nitrogen atom, which has been observed before in the X-ray structure of the phosphoramidite ligand **5c**.[29] Details are discussed below together as are the other structures obtained for this study.

Allenylidene Complex Synthesis

As only **12b** and **12c** were obtained with diastereomeric purity, they were employed in allenylidene complex synthesis under the conditions previously described for the synthesis of the related allenylidene complex $[Ru(Ind)(PPh_3)_2(=C=C=CPh_2)]^+[PF_6]^-$ (**13**).[41] However, the use of $NaPF_6$ in MeOH at reflux[41] with complex **12b** and propargylic alcohol **14a** resulted in a sluggish reaction generating a 1:1 mixture of diastereomers, as revealed by NMR (^1H, ^{31}P). When $AgPF_6$ in CH_2Cl_2 was used for chloride abstraction followed by filtration to remove AgCl, the corresponding allenylidene complex was obtained with diastereomeric purity. However, we found that the chloride scavenger $(Et_3O)PF_6$ can also be used for activation of the precursor complexes **12b** and **12c**. By using $(Et_3O)PF_6$ for chloride ab-

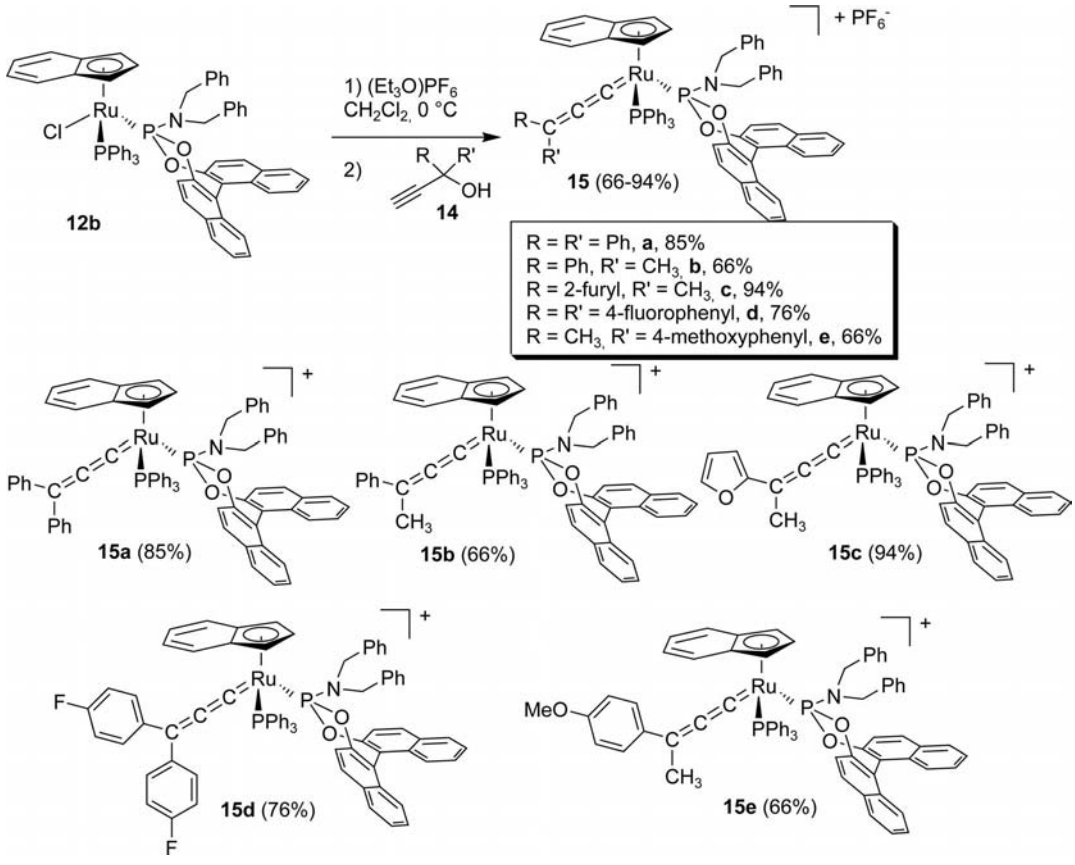

Scheme 4. Synthesis of allenylidene complexes.

straction, the removal of MCl was not necessary, facilitating the work-up.

Accordingly, a CH_2Cl_2 solution of complex **12b** was first treated at 0 °C with 1 equiv. of $(Et_3O)PF_6$, which resulted in a slight darkening of the solution (Scheme 4). The corresponding propargylic alcohol **14** was subsequently added, which resulted in a quick color change from red to dark purple. After removal of all the volatiles and washing with Et_2O, the novel phosphoramidite complexes [**15a**–**e**]$^+$ were isolated as their PF_6^- salts as intensely colored purple powders in 66–94% isolated yields. These complexes will subsequently be referred to without charges and counterions.

The new allenylidene complexes **15** were characterized by NMR (^{1}H, ^{13}C, ^{31}P), MS, IR, and elemental analysis. Their formation was best demonstrated by the characteristic signals in the IR and ^{13}C NMR spectra. As generally observed for allenylidene complexes,[1f] the carbon atoms of the allenylidene chain give distinct resonances of low intensity in the ^{13}C NMR spectra for the C_α (293.8–299.4 ppm), C_β (185.2–199.7 ppm), and C_γ (159.9–162.8 ppm) carbons. The C_α resonance appears as a doublet, a doublet of doublets (J_{CP} = 20.8–23.6 Hz), or a multiplet due to C–P couplings. The resonances for C_β in **15b** also show J_{CP} coupling (13.8 Hz). Furthermore, the new complexes give an intense band for the allenylidene chain in the IR spectra between 1935 and 1949 cm^{-1}, which is also indicative of this class of complexes.[1f]

In the ^{31}P NMR spectra, the signals arising from the PPh_3 and phosphoramidite ligands in **15** are slightly shifted relative to those of the corresponding starting materials. Most significantly, only one set of signals was observed in all the NMR spectra of both crude and isolated material, which suggests that only one diastereomer was formed. No vinylic resonances were observed in the ^{1}H NMR spectra of **15b**,**c**,**e**, which suggests that no vinylvinylidene isomers were present in the isolated material and thus no isomerization took place, as sometimes reported when Selegue's protocol is applied to allenylidene synthesis (see below).[1a,30] The allenylidene complexes **15** are air-stable powders; complex **15c** is somewhat hygroscopic and was isolated as a hydrate, as shown by ^{1}H NMR, IR, and elemental analysis.

To unequivocally establish the structures and configurations of the novel allenylidene complexes, the X-ray structures of complexes **15a**,**b**,**d** were determined (Tables 1 and 2, Figure 3). The solid-state structures show that the absolute configurations about the ruthenium center in **12b** and **15a**,**b**,**d** are identical. The chloro ligand is replaced by the allenylidene chain with overall retention of the absolute

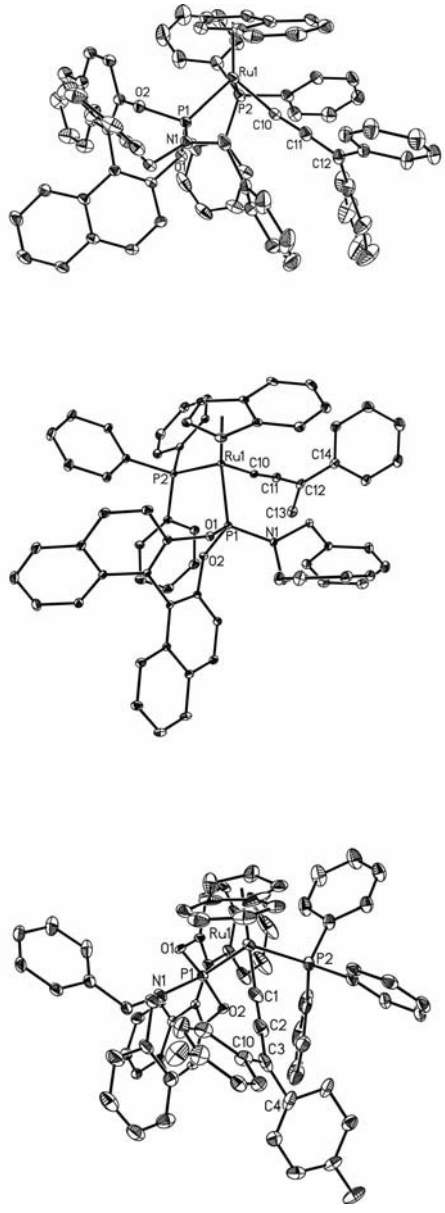

Figure 3. Molecular Structures of **15a** (top), **15b** (middle), and **15d** (bottom). Ellipsoids are shown at the 30% probability level. Hydrogen atoms and solvent molecules have been omitted for clarity. For key bond lengths and angles, see Table 1.

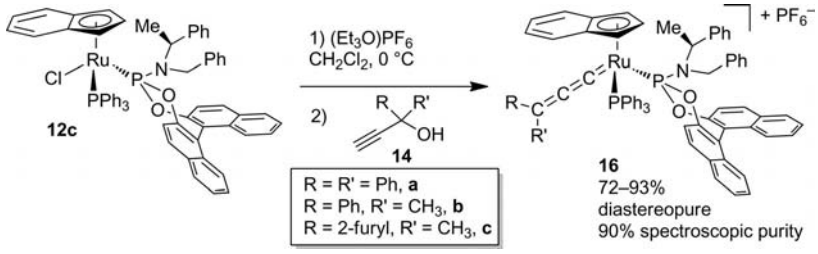

Scheme 5. Synthesis of less stable allenylidene complexes.

configuration and the chiral information has been transferred from the starting material **12b** to the products **15a**,**b**,**d**. The structures will be discussed in more detail in the next section.

The precursor complex **12c** could also be converted into the corresponding allenylidene complexes by using the same protocol as employed for the synthesis of complexes **15** (Scheme 5). The resulting allenylidene complexes **16a**–**c** were isolated in 72–93% yields with approximately 90% spectroscopic purity, but attempts at purification resulted in ongoing decomposition. The NMR, IR, and MS characterization data (which are given in the Supporting Information) are similar to those of complexes **15** and clearly show the formation of allenylidene complexes in diastereopure form. However, complexes **16b** and **16c** decomposed within hours in $CDCl_3$, as can be seen by the appearance of extra peaks in the ^{13}C NMR spectra. Complexes **16** appear to be hygroscopic as the presence of water is observed in the ^1H NMR spectra and elemental analyses. We hypothesize that the extra methyl group on the carbon atom in the position α to the nitrogen creates significant steric congestion about the ruthenium center, which destabilizes the corresponding complexes leading to PPh_3 dissociation.

Further Experiments Related to the Stereochemistry of the New Complexes

The chloro precursor complexes **12b** and **12c** and all the allenylidene complexes **15** and **16** were obtained as enantiopure single diastereomers. NMR evidence of a second diastereomer was not observed for any of the precursors or allenylidene complexes. To obtain further information about the configurational stability of the complexes as well as the diastereoselective formation of the allenylidenes, dynamic NMR experiments were performed with the chloro precursor **12b** and allenylidene complex **15a**.

Both complexes **12b** and **15a** showed configurational stability between –50 and +25 °C, as indicated by their ^1H and ^{31}P NMR spectra (see the Supporting Information), which exhibit only minor line-broadening at different temperatures. The precursor complex **12b** is configurationally stable up to 60 °C, whereas the allenylidene complexes **15** and **16** show significant decomposition at elevated temperatures.

To obtain information about the diastereoselective formation of the allenylidene complexes, a dynamic NMR experiment was performed. A sample of the chloro precursor complex **12b** was first treated with $(Et_3O)PF_6$ and ^1H and ^{31}P NMR spectra were recorded at different temperatures. Subsequently, the propargylic alcohol **14a** was added to the same sample, and again ^1H and ^{31}P NMR spectra were recorded. All the NMR spectra are given in the Supporting Information and Figure 4 shows the three ^{31}P NMR spectra recorded at –30 °C.

It appears that abstraction of the chloride from the precursor complex **12b** (Figure 4, top) results in a species **17** (Figure 4, middle), which shows some dynamic behavior in solution. A second set of doublets appears, which might be due to a second diastereomer formed in solution (at +25 °C, only two very broad peaks at around 175 and 45 ppm were observed, see the Supporting Information). Upon addition of the propargylic alcohol, only one set of signals for the product was observed in the ^{31}P NMR spectrum (Figure 4, bottom). These spectra show that only one of the two possible diastereomers of the allenylidene complex forms during the reaction.

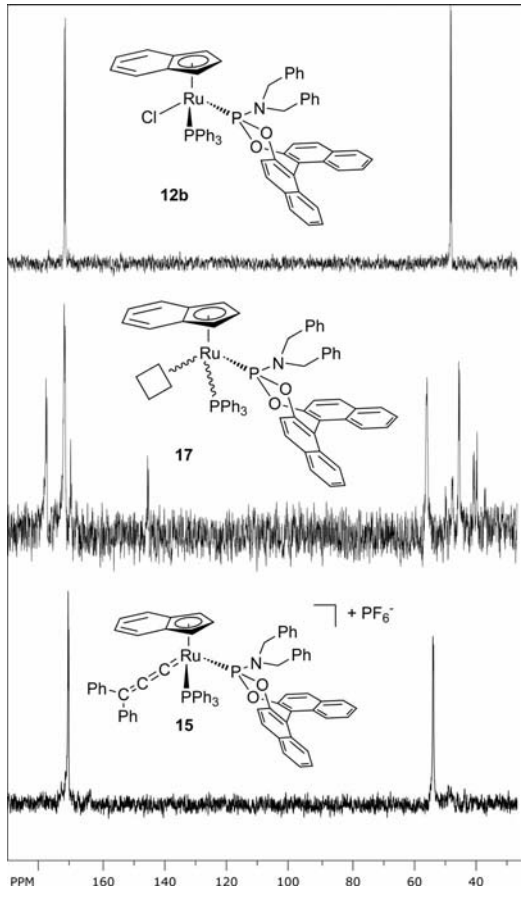

Figure 4. ^{31}P NMR spectra recorded at –30 °C for different steps in allenylidene formation. Top: starting complex **12b**. Middle: spectrum recorded immediately after the addition of $(Et_3O)PF_6$. Bottom: spectrum recorded immediately after the addition of propargylic alcohol **14a**.

A potential second diastereomer could result from an exchange of the two phosphorus-based ligands to give a mixture of **17a** and **17b** (Scheme 6). Assuming a dynamic process at the metal, species **17a** in Scheme 6 must react with the propargylic alcohol much faster than species **17b** to produce the observed diastereoselectivity. However, it has been reported in the literature that extra signals in the NMR spectra of the corresponding complexes may appear at low temperatures due to slowing of dynamic processes centered on the ligands.[19b] In the free ligand **5c**, dynamic NMR experiments have shown that rotation around the P–N bond is frozen at –70 °C.[29]

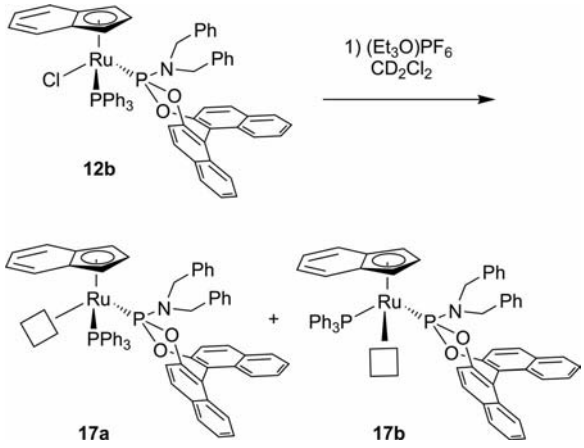

Scheme 6. NMR tube experiment. The square denotes an open coordination site.

Discussion

Scope of the Reaction

This report describes the synthesis and structural characterization of the first ruthenium phosphoramidite allenylidene complexes. The new complexes are chiral at the metal and were obtained from the corresponding chloro precursors with chirality transfer, as determined by the X-ray structures of the complexes **12b** and **15a**,**b**,**d**. Both electron-rich (**14e**) and electron-poor (**14d**) propargylic alcohols bearing either two aryl groups (**14a**,**d**) or one aryl and one alkyl group (**14b**,**c**,**e**) could be employed in the synthesis of the complexes (Scheme 4). Purely aliphatic propargylic alcohols failed to be converted into the corresponding allenylidenes, which is in accord with the general observation in the literature that aliphatic allenylidene complexes are less stable than those bearing at least one aryl substituent at the γ carbon.[1] Interestingly, we did not observe any vinylvinylidene species, which often form when a propargylic alcohol with α protons on the γ substituent are employed (Scheme 7).[30] In that case, dehydration of the intermediate **18** can, in addition to the allenylidene complex, give the corresponding vinylvinylidene species **19**. We hypothesize that for steric reasons, the formation of the bent vinylvinylidene chain in **19** is disfavored. The coordination sphere about the ruthenium center in the allenylidene complexes **15** is very congested and a bent vinylvinylidene chain is sterically more demanding than a straight allenylidene chain. We also did not observe allenylidene-to-indenylidene rearrangements,[31] which would also increase steric demand about the ruthenium center.

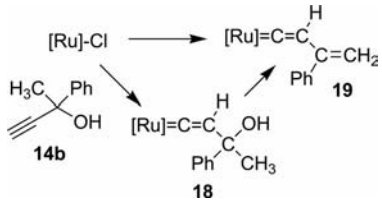

Scheme 7. Potential vinylvinylidene formation.

X-ray Crystallography

The X-ray analyses of **12b** and **15a**,**b**,**d** confirm the proposed piano-stool structures of the complexes. Key bond lengths and angles are compiled in Table 1 and, for comparison, the corresponding values for the structurally related complex $[Ru(Ind)(PPh_3)_2(=C=C=CPh_2)]PF_6$ (**13**) are also listed.[41] The bond angles about the ruthenium center range from 84.81(6) to 92.73(7)°. The structures are thus best described as slightly distorted octahedra. In all three complexes, the Ru–P bond lengths for the phosphoramidite ligands are shorter than those for the PPh_3 ligands, with Ru–P1 ranging from 2.1961(7) to 2.2730(6) Å compared with the Ru–P2 bond lengths of 2.3037(5) to 2.3504(8) Å, respectively. We observed this phenomenon previously in the X-ray structures of complexes of **6** (Figure 1).[23] As a result of the oxygen atoms bonded to the phosphorus, the phosphoramidite ligands might be somewhat more π-acidic than PPh_3. This could result in a higher degree of metal-to-ligand back-bonding, which would shorten the Ru–P bond.

As reported for ligand **5c**,[29] ligand **5b** features an almost planar nitrogen atom, as seen by the calculated average deviation from planarity involving the nitrogen and the two carbon and one phosphorus atom bonded to it [Table 1 and Equation (1)]. We ascribed the planarity tentatively to a partial double-bond character of the P–N bond. Interestingly, the free ligand deviates from planarity slightly more (0.0305 Å) than the coordinated ligand (0.0045–0.0281 Å). Upon coordination of the phosphoramidite ligand, resonance structure **21** in Equation (1) may contribute significantly to the various resonance structures of ligand **5b**, increasing the double-bond character of the P–N bond and hence the planarity about the nitrogen atom.

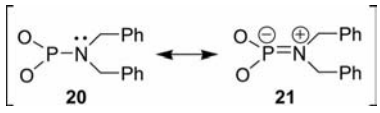

(1)

There are slight structural differences between the allenylidene complexes **15a**,**b**,**d** and **13**, which mainly concern the geometry about the ruthenium center. The P1–Ru–P2 bond angles for **15a**,**b**,**d** are about 3° larger than for **13**, as expected for the bulkier phosphoramidite ligands. The bond lengths about the ruthenium center for the phosphoramidite complexes **15a** and **15b** are slightly smaller than for **13**, which could be associated with greater π-acidity of the phosphoramidite ligands.

The C10–C11–C12 angles of the allenylidene chain in **15a**,**b**,**d** are 177.6(3), 174.9(2), and 174.8(5)°, respectively. This slight deviation from the ideal angle of 180° has frequently been observed for other allenylidene complexes.[1] The angles between C11, C12, and the *ipso* atom of the

substituent at C12 are between 120.1(3) and 124.8(8)°, which confirms the sp^2 hybridization of the C_γ atom of the allenylidene chain. The C=C bonds of the allenylidene chain are not of equal length in the three complexes. The internal C_α=C_β bond is significantly shorter [1.250(3)–1.256(6) Å] than the terminal C_β=C_γ bond [1.346(7)–1.357(4) Å]. Such bond differences are frequently observed in allenylidene complexes[1a] and they can be explained by the resonance contributor **B**, which exhibits an internal triple bond and results in a significantly shorter bond length in the X-ray analysis; see Equation (2).

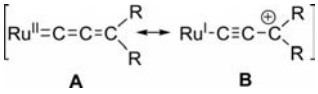

(2)

The position of the indenyl ligand relative to the other three ligands in the solid-state structures is schematically shown in Figure 5. As can be seen in **C**, for the chloro complex **12b** the aryl ring of the indenyl ligand occupies the interstitial site between the chloro and the PPh_3 ligands. This conformation might be ascribed to steric factors as it is the largest of the three potential interstitial sites. However, in the corresponding allenylidene complexes **15a** and **15b**, the position of the three ligands relative to the indenyl ring has changed. Now, the aryl ring of the indenyl ligand is oriented along the allenylidene chain, represented as **D** in Figure 5. The same orientation was observed in the structurally related complex **13**.[4l] This orientation might have an impact on the potential attack of nucleophiles as the electrophilic C_α carbon atom is sterically much more protected than the C_γ carbon.

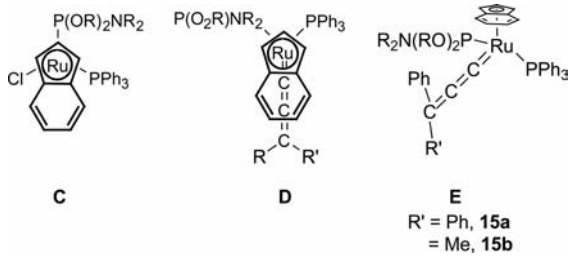

Figure 5. Schematic representation of the conformations of the chloro and allenylidene complexes.

The positions of the two substituents at the C_γ carbon atom in the allenylidene complexes (two aryls in **15a** and one phenyl and one methyl in **15b**) is schematically represented by **E** (Figure 5). The substituents are oriented almost in a plane with an axis formed by the C_α atom of the allenylidene chain, the ruthenium center, and the cyclopentadienyl centroid of the indenyl ligand. However, some deviation from this planar alignment was observed, which has also been described for complex **13**.[4l] This deviation can be quantified by the angle between the planes defined by the Cp centroid, Ru, and C10 and C10–C11–C12–C13 or C1–C2–C3–C4 (dihedral angle in Table 1)[4l] and is 34.4° for **15a**, 14.8° for **15b**, 27.6° for **15d**, and 15.5(3)° for **13**. For **15b**, the phenyl ring points upwards and the methyl substituent points downwards relative to the indenyl ligand. It has previously been suggested that the C_γ substituents are aligned in such a way as to maximize the overlap between the d π HOMO of the metal and the p π LUMO of the allenylidene chain, allowing for maximized metal-to-ligand back-donation.[1a,32]

As can be seen in the schematic representation **D** in Figure 5, the allenylidene chain is flanked by the phosphoramidite ligand to the left and the PPh_3 ligand to the right. Nucleophilic attack on the C_γ carbon as shown in Scheme 1 can either take place from the left or the right side in **D** and as consequence of the chirality at the metal the two faces are inequivalent. Figure 6 shows selected atoms of the X-ray structure of **15b**. It shows that one side of C_γ is shielded by the phosphoramidite ligand much more efficiently than the other side is shielded by the PPh_3 ligand. The distance of the C_γ carbon atom to the centroid of the closest phenyl ring of the PPh_3 ligand is 4.97 Å (dotted line in Figure 6, calculated with the Mercury 1.4.2 software[40]), whereas it is 3.80 Å for the centroid of the closest phenyl ring of the phosphoramidite ligand. This difference potentially allows for stereodifferentiation upon attack of the C_γ atom by a nucleophile. Stoichiometric and catalytic experiments to take advantage of this situation in propargylic substitution reactions (as exemplified in Scheme 1) are currently underway.

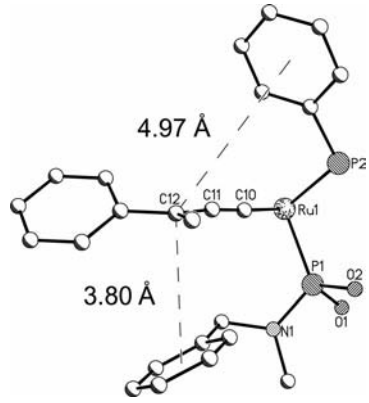

Figure 6. Shielding of the C_γ carbon atom by the ligands.

Conclusions

We have synthesized the first ruthenium allenylidene complexes bearing chiral phosphoramidite ligands in the coordination sphere. The new allenylidene complexes are chiral at the metal and were obtained as optically pure single diastereomers from the corresponding chloro precursor complexes. The chloro ligand was replaced with the allenylidene chain with complete transfer of chirality. The results presented herein may have an impact on the catalytic applications of allenylidene complexes both as chiral catalysts and chiral reactive intermediates in propargylic substitution reactions. Corresponding studies are underway.

Experimental Section

General Methods: Chemicals were treated as follows: THF, toluene, and diethyl ether (Et_2O) were distilled from Na/benzophenone, CH_2Cl_2 was distilled from CaH_2. (*R*)-1,1′-Binaphthyl-2,2′-diol [(*R*)-binol] (Strem), catechol (Fisher), phosphorus trichloride (PCl_3), *N*-methyl-2-pyrrolidinone (Acros), (*R*)-2-methylpyrrolidine (Aldrich), 1,1-diphenyl-2-propyn-1-ol (Aldrich), 2-phenyl-3-butyn-2-ol (Aldrich), ($Et_3O)PF_6$ (Aldrich), Celite® (Aldrich), *tert*-butyl methyl ether (Aldrich), and other materials were used as received. (*R*)-binol-*N*,*N*-dimethylphosphoramidite (**5a**),[21a] (*R*)-binol-*N*,*N*-dibenzylphosphoramidite (**5b**),[21c] (*R*,*S*)-binol-*N*-benzyl-*N*-α-methylbenzylphosphoramidite (**5c**),[33] 2-(2-furyl)-3-butyn-2-ol (**14c**),[34] bis(4-fluorophenyl)-3-propyn-2-ol (**14d**),[35a] 2-(4-methoxyphenyl)-3-butyn-2-ol (**14e**),[35b] and [RuCl(Ind)($PPh_3)_2$] (**11**)[28] were synthesized according to literature procedures.

NMR spectra were recorded at room temperature with a Bruker Avance 300 MHz or Varian Unity Plus 300 MHz instrument and referenced to a residual solvent signal. All assignments are tentative. Exact masses were obtained with a JEOL MStation [JMS-700] mass spectrometer. Melting points were measured with an Electrothermal 9100 instrument. IR spectra were recorded with a Thermo Nicolet 360 FT-IR spectrometer. Elemental analyses were performed by Atlantic Microlab Inc., Norcross, GA, USA.

(*R*)-Catechol-2-methylpyrrolidine-phosphoramidite [(*R*)-10]: Phosphorus trichloride (PCl_3; 2.0 mL, 23 mmol) was added to a Schlenk flask containing catechol (0.402 g, 3.65 mmol) followed by *N*-methyl-2-pyrrolidinone (0.01 mL, 0.1 mmol). The resulting slurry was heated at reflux for 30 min. Excess PCl_3 was removed under oil-pump vacuum to yield a yellow liquid. Et_2O (5.0 mL) was added and removed under vacuum twice to remove remaining PCl_3. The liquid was dissolved in THF (12 mL) and triethylamine was added (0.83 mL, 6.3 mmol) followed by (*R*)-2-methylpyrrolidine (0.32 mL, 3.2 mmol). After stirring for 1 h at room temperature, the resulting slurry was filtered through Celite® and the solvent removed under vacuum. The yellow liquid was dissolved in CH_2Cl_2 (30 mL) and extracted with saturated aq. $NaHCO_3$ (2 × 30 mL). The organic layer was dried with Na_2SO_4, filtered, and the volatiles removed under oil-pump vacuum to yield (*R*)-**10** as a yellow oil (0.569 g, 2.55 mmol, 78%). ^{1}H NMR (300 MHz, $CDCl_3$, 25 °C): δ = 6.92–6.84 (m, 2 H, Ph), 6.82–6.75 (m, 2 H, Ph), 3.79–3.63 (m, 1 H, NC*H*CH_3), 2.92–2.73 (m, 2 H, NCH_2), 1.90–1.78 (m, 1 H, C*H*H′), 1.77–1.52 (m, 2 H, CH_2), 1.41–1.29 (m, 1 H, CH*H*′), 1.11 (d, $^3J_{HH}$ = 6.4 Hz, 3 H, CH_3) ppm. ^{13}C{^{1}H} NMR (75 MHz, $CDCl_3$, 25 °C): δ = 146.8 (d, $^2J_{CP}$ = 8.1 Hz, CO), 146.6 (d, $^2J_{CP}$ = 8.1 Hz, C′O), 122.0 (s, Ph), 111.5 (s, Ph), 54.5 (d, $^2J_{CP}$ = 22.2 Hz, NCH), 44.3 (d, $^2J_{CP}$ = 4.1 Hz, NCH_2), 34.6 (d, $^3J_{CP}$ = 3.5 Hz, CH_2), 24.9 (d, $^3J_{CP}$ = 1.6 Hz, CH_2), 24.0 (d, $^3J_{CP}$ = 8.3 Hz, CH_3) ppm. ^{31}P{^{1}H} NMR (121 MHz, $CDCl_3$, 25 °C): δ = 145.0 (s) ppm. IR (neat solid): $\tilde{\nu}$ = 3061 (m), 2966 (s), 2871 (s), 1604 (m), 1483 (s), 1335 (s), 1240 (s), 859 (s), 745 (s) cm^{-1}. HRMS: calcd. for $C_{11}H_{14}NO_2P$ 223.0762; found 223.0755. $C_{11}H_{14}NO_2P$ (223.21): calcd. C 59.19, H 6.32; found C 58.90, H 6.31.

[RuCl(Ind)(PPh_3)(5a)] (12a): Toluene (5 mL) was added to a Schlenk flask containing [RuCl(Ind)($PPh_3)_2$] (**11**; 0.218 g, 0.281 mmol) and phosphoramidite **5a** (0.101 g, 0.281 mmol) and the mixture was heated at 65 °C in an oil bath for 2 h. The solvent was removed under vacuum and the resulting solid was purified by flash chromatography employing a 2 × 15 cm silica column. The remaining ligand and PPh_3 were eluted with CH_2Cl_2 and then the complex was eluted with CH_2Cl_2/*tert*-butyl methyl ether (9:1, v/v), collecting the red band. The solvent was removed under vacuum to give **12a** as an orange solid in a 2:1 diastereomeric mixture (0.195 g, 0.223 mmol, 79%); m.p. 148–149 °C (dec., capillary). ^{1}H NMR (300 MHz, $CDCl_3$, 25 °C):[36] δ = 7.90–7.66 (m, 6 H, arom.), 7.52 (d, $^3J_{HH}$ = 4.3 Hz, 2 H, arom.), 7.45–7.08 (m, 18 H, arom.), 7.06–6.95 (m, 5 H, arom.), 6.92–6.80 (m, 14 H, arom.), 6.73 (t, $^3J_{HH}$ = 7.2 Hz, 1 H, arom.), 6.55 (d, $^3J_{HH}$ = 8.3 Hz, 1 H, arom.), 5.47–5.40 (m, 1 H, indenyl), 5.28 (br. s, 1 H, indenyl), 4.97 (br. s, 0.5 H, indenyl*), 4.63 (br. s, 0.5 H, indenyl*), 4.18 (br. s, 1 H, indenyl), 3.71 (br. s, 0.5 H, indenyl*), 2.47 (s, 3 H, CH_3), 2.43 (s, 3 H, CH_3′), 1.92 (br. s, 1.5 H, CH_3*), 1.89 (br. s, 1.5 H, CH_3′*) ppm. ^{13}C{^{1}H} NMR (75 MHz, $CDCl_3$, 25 °C; major diastereomer):[37] δ = 153.2 (s, arom.), 150.9 (d, J_{CP} = 14.7 Hz, arom.), 149.6 (d, J_{CP} = 8.0 Hz, arom.), 136.7 (s, arom.), 136.1 (s, arom.), 134.6 (d, J_{CP} = 10.5 Hz, arom.), 134.2 (d, J_{CP} = 10.0 Hz, arom.), 133.4 (s, arom.), 133.1 (s, arom.), 131.3 (s, arom.), 131.2 (d, J_{CP} = 3.7 Hz, arom.), 130.2 (s, arom.), 129.8 (s, arom.), 129.4 (br. s, arom.), 128.8 (s, arom.), 128.6 (d, J_{CP} = 3.3 Hz, arom.), 128.4 (s, arom.), 128.3 (s, arom.), 128.2 (s, arom.), 128.1 (s, arom.), 127.8 (s, arom.), 127.7 (s, arom.), 127.6 (s, arom.), 127.4 (s, arom.), 127.2 (s, arom.), 127.1 (s, arom.), 126.2 (s, arom.), 126.0 (s, arom.), 125.2 (d, J_{CP} = 4.2 Hz, arom.), 125.0 (s, arom.), 124.8 (s, arom.), 124.0 (s, arom.), 123.9 (s, arom.), 123.0 (d, J_{CP} = 3.3 Hz, arom.), 122.0 (s, arom.), 118.3 (s, arom.), 113.0 (d, J_{CP} = 5.5 Hz, indenyl), 112.2 (d, J_{CP} = 5.9 Hz, indenyl), 91.4 (s, indenyl), 66.9 (d, J_{CP} = 9.7 Hz, indenyl), 63.3 (s, indenyl), 39.5 (s, CH_3), 39.4 (CH_3′) ppm. ^{31}P{^{1}H} NMR (121 MHz, $CDCl_3$, 25 °C): δ = 177.5 (br. s, phosphoramidite*), 176.3 (d, $^2J_{PP}$ = 65.1 Hz, phosphoramidite), 52.1 (br. s, PPh_3*), 49.2 (d, $^2J_{PP}$ = 65.1 Hz, PPh_3) ppm. IR (neat solid): $\tilde{\nu}$ = 3047 (w), 2917 (w), 1586 (w), 1432 (m), 1223 (m), 945 (m), 693 (m) cm^{-1}. HRMS: calcd. for $C_{49}H_{40}NO_2P_{235}Cl^{102}Ru$ 873.1265; found 873.1284.

[RuCl(Ind)(PPh_3)(5b)] (12b): THF (8 mL) was added to a Schlenk flask containing [RuCl(Ind)($PPh_3)_2$] (**11**; 0.303 g, 0.390 mmol) and phosphoramidite **5b** (0.200 g, 0.391 mmol) and the solids dissolved. The red solution was heated at reflux in an oil bath for 1 h. The solvent was removed under vacuum and the resulting solid was purified by flash chromatography employing a 2.5 × 15 cm silica column. The remaining ligand and PPh_3 were eluted with CH_2Cl_2 and then the complex was eluted with CH_2Cl_2/Et_2O (99:1, v/v), collecting the red band. The solvent was removed under vacuum to give **12b** as a single diastereomer (0.347 g, 0.338 mmol, 87%); m.p. 176–177 °C (dec., capillary). ^{1}H NMR (300 MHz, $CDCl_3$, 25 °C): δ = 8.11 (t, $^3J_{HH}$ = 8.3 Hz, 2 H, arom.), 7.70 (d, $^3J_{HH}$ = 8.1 Hz, 1 H, arom.), 7.62 (d, $^3J_{HH}$ = 8.4 Hz, 1 H, arom.), 7.54 (t, $^3J_{HH}$ = 7.1 Hz, 1 H, arom.), 7.52–7.44 (m, 2 H, arom.), 7.35–7.20 (m, 14 H, arom.), 7.15–6.84 (m, 12 H, arom.), 6.75 (d, $^3J_{HH}$ = 8.8 Hz, 3 H, arom.), 6.50–6.35 (m, 5 H, arom.), 5.71 (br. s, 1 H, indenyl), 5.36 (br. s, 1 H, indenyl), 5.00 (d, $^2J_{HH}$ = 10.6 Hz, 1 H, NC*H*H′), 4.95 (d, $^2J_{HH}$ = 10.6 Hz, 1 H, NCH*H*′), 4.05 (br. s, 1 H, indenyl), 3.54 (d, $^2J_{HH}$ = 15.1 Hz, 1 H, NC*H*H′), 3.49 (d, $^2J_{HH}$ = 15.1 Hz, 1 H, NCH*H*′) ppm. ^{13}C{^{1}H} NMR (75 MHz, $CDCl_3$, 25 °C): δ = 151.3 (s, arom.), 151.1 (s, arom.), 149.2 (s, arom.), 148.5 (s, arom.), 139.4 (s, arom.), 134.3 (br. s, arom.), 133.8 (s, arom.), 132.7 (s, arom.), 131.5 (s, arom.), 131.1 (s, arom.), 130.2 (s, arom.), 130.0 (s, arom.), 129.5 (s, arom.), 128.6 (s, arom.), 128.4 (s, arom.), 127.2 (s, arom.), 126.2 (s, arom.), 125.8 (s, arom.), 125.5 (s, arom.), 125.0 (s, arom.), 124.4 (s, arom.), 123.3 (s, arom.), 122.8 (s, arom.), 122.0 (s, arom.), 121.4 (s, arom.), 113.6–113.5 (m, indenyl), 111.8–111.7 (m, indenyl), 90.4 (s, indenyl), 67.1 (d, $^2J_{CP}$ = 10.8 Hz, indenyl), 62.0 (s, indenyl), 50.6 (s, NCH_2), 50.5 (s, NCH_2) ppm. ^{31}P{^{1}H} NMR (121 MHz, $CDCl_3$, 25 °C): δ = 172.8 (d, $^2J_{PP}$ = 58.5 Hz, phosphoramidite), 46.8 (d, $^2J_{PP}$ = 58.5 Hz, PPh_3) ppm. IR (neat solid): $\tilde{\nu}$ = 3050 (w), 1586 (w), 1223 (m), 940 (m), 741 (m), 692 (m) cm^{-1}. HRMS: calcd. for $C_{61}H_{48}ClNO_2P_{235}{}^{102}Ru$

1025.1892; found 1025.1924. $C_{61}H_{48}ClNO_2P_2Ru$ (1025.51): calcd. C 71.44, H 4.72; found C 71.44, H 4.66.

[RuCl(Ind)(PPh$_3$)(5c)] (12c): THF (10 mL) was added to a Schlenk flask containing [RuCl(Ind)(PPh$_3$)$_2$] (**11**; 0.442 g, 0.569 mmol) and phosphoramidite **5c** (0.299 g, 0.570 mmol) and the solids dissolved. The red solution was heated at reflux for 3 h. The solvent was removed under vacuum and the resulting solid was purified by flash chromatography employing a 2 × 16 cm silica column. The remaining ligand and PPh$_3$ were eluted with CH_2Cl_2 and then the complex was eluted with CH_2Cl_2/Et_2O (99:1, v/v), collecting the red band. The solvent was removed under vacuum to give **12c** as a single diastereomer (0.471 g, 0.453 mmol, 80%); m.p. 162–164 °C (dec., capillary). ^{1}H NMR (300 MHz, $CDCl_3$, 25 °C): δ = 7.98 (d, $^3J_{HH}$ = 8.9 Hz, 2 H, arom.), 7.62–7.55 (m, 4 H, arom.), 7.43 (t, $^3J_{HH}$ = 7.2 Hz, 1 H, arom.), 7.35–7.29 (m, 5 H, arom.), 7.27–7.25 (m, 2 H, arom.), 7.20–7.01 (m, 9 H, arom.), 7.00–6.85 (m, 7 H, arom.), 6.80–6.72 (m, 4 H, arom.), 6.62–6.58 (br. m, 2 H, arom.), 6.44 (d, $^3J_{HH}$ = 8.9 Hz, 1 H, arom.), 6.33–6.22 (br. m, 4 H, arom.), 6.19 (d, $^3J_{HH}$ = 8.4 Hz, 1 H, arom.), 5.81–5.79 (m, 1 H, indenyl), 5.57 (br. s, 1 H, indenyl), 3.98 (br. s, 1 H, indenyl), 3.90–3.81 (m, 1 H, C*H*H′), 3.22–3.13 (m, 1 H, CH*H*′), 1.07 (d, $^3J_{HH}$ = 7.2 Hz, 3 H, CH_3) ppm.[38] ^{13}C{^{1}H} NMR (75 MHz, $CDCl_3$, 25 °C): δ = 151.4 (s, arom.), 151.2 (s, arom.), 143.2 (d, J_{CP} = 8.1 Hz, arom.), 142.8 (s, arom.), 137.9 (s, arom.), 137.5 (s, arom.), 137.4 (s, arom.), 137.0 (s, arom.), 135.7 (d, J_{CP} = 39.9 Hz, arom.), 134.2 (s, arom.), 133.7 (s, arom.), 133.2 (s, arom.), 133.1 (s, arom.), 132.7 (s, arom.), 131.4 (s, arom.), 131.0 (s, arom.), 130.1 (s, arom.), 129.7 (s, arom.), 129.2 (s, arom.), 128.7 (s, arom.), 128.5 (d, J_{CP} = 24.0 Hz, arom.), 128.3 (d, J_{CP} = 18.0 Hz, arom.), 128.1 (s, arom.), 128.0 (s, arom.), 127.2 (s, arom.), 127.1 (s, arom.), 126.5 (s, arom.), 126.3 (s, arom.), 126.0 (s, arom.), 125.7 (d, J_{CP} = 26.1 Hz, arom.), 124.9 (s, arom.), 123.9 (s, arom.), 122.9 (s, arom.), 122.7 (s, arom.), 122.0 (s, arom.), 121.3 (s, arom.), 114.3 (d, J_{CP} = 18.0 Hz, indenyl), 113.0 (d, J_{CP} = 24.0 Hz, indenyl), 90.4 (s, indenyl), 68.3 (d, $^2J_{CP}$ = 48.0 Hz, indenyl), 59.1 (s, indenyl), 54.9 (d, $^2J_{CP}$ = 68.1 Hz, NC), 49.0 (s, NC′), 21.7 (d, $^3J_{CP}$ = 21.9 Hz, CH_3) ppm. ^{31}P{^{1}H} NMR (121 MHz, $CDCl_3$, 25 °C): δ = 172.0 (d, $^2J_{PP}$ = 58.6 Hz, phosphoramidite), 45.9 (d, $^2J_{PP}$ = 58.6 Hz, PPh$_3$) ppm. IR (neat solid): $\tilde{\nu}$ = 3051 (w), 2927 (w), 1584 (w), 1430 (m), 1221 (m), 949 (s) cm^{-1}. HRMS: calcd. for $C_{62}H_{50}ClNO_2P_{235}{}^{102}Ru$ 1039.2048; found 1039.2004. $C_{62}H_{50}ClNO_2P_2Ru$ (1039.54): calcd. C 71.63, H 4.85; found C 71.04, H 4.84.

[RuCl(Ind)(PPh$_3$){(*R*)-10}] (12d): Phosphoramidite (*R*)-**10** (0.032 g, 0.14 mmol) was added as a solution in toluene (3 mL) to a Schlenk flask containing [RuCl(Ind)(PPh$_3$)$_2$] (**11**; 0.109 g, 0.141 mmol). The mixture was heated at 65 °C for 2 h in an oil bath after which the solvent was removed under oil-pump vacuum. The resulting red solid was purified by flash chromatography employing a 1 × 11 cm silica column. The remaining ligand and PPh$_3$ were eluted with CH_2Cl_2 and then the complex was eluted with CH_2Cl_2/*tert*-butylmethyl ether (9:1, v/v), collecting the red band. The solvent was removed under oil-pump vacuum to give complex **12d** as an orange solid in a 1:1 diastereomeric mixture (0.069 g, 0.094 mmol, 67%); m.p. 99–100 °C (dec., capillary). ^{1}H NMR (300 MHz, $CDCl_3$, 25 °C):[36] δ = 7.74–7.57 (m, 2 H, arom.), 7.33–6.94 (m, 34 H, arom.), 6.90–6.73 (m, 3 H, arom.), 6.73–6.57 (m, 3 H, arom.), 6.51–6.37 (m, 2 H, arom.), 6.00–5.85 (m, 2 H, arom.), 5.09 (br. s, 1 H, indenyl), 4.92 (br. s, 2 H, indenyl), 4.69 (br. s, 1 H, indenyl), 4.31 (br. s, 1 H, indenyl), 4.01 (br. s, 1 H, indenyl), 3.89–3.79 (m, 1 H, NC*H*CH$_3$), 3.79–3.69 (m, 1 H, NC*H*CH$_3$*), 3.45–3.32 (m, 1 H, NC*H*H′), 3.21–3.08 (m, 1 H, NC*H*H′*), 2.91–2.80 (m, 1 H, NCH*H*′), 2.78–2.65 (m, 1 H, NCH*H*′*), 1.89–1.57 (m, 5 H, 2 CH_2, C*H*H′), 1.57–1.44 (m, 1 H, C*H*H′*), 1.37–1.23 (m, 2 H, 2 CH*H*′), 0.96 (d, $^3J_{HH}$ = 6.4 Hz, 3 H, CH_3), 0.81 (d, $^3J_{HH}$ = 6.4 Hz, 3 H, CH_3*) ppm. ^{13}C{^{1}H} NMR (75 MHz, $CDCl_3$, 25 °C): δ = 148.2 (d, J_{CP} = 5.6 Hz, arom.), 147.6 (d, J_{CP} = 6.9 Hz, arom.), 147.0 (d, J_{CP} = 5.0 Hz, arom.), 146.1 (d, J_{CP} = 5.6 Hz, arom.), 136.8 (s, arom.), 136.5 (s, arom.), 136.1 (s, arom.), 135.9 (s, arom.), 134.2 (d, J_{CP} = 2.7 Hz, arom.), 134.1 (d, J_{CP} = 2.1 Hz, arom.), 129.5 (d, J_{CP} = 2.2 Hz, arom.), 129.4 (d, J_{CP} = 2.2 Hz, arom.), 128.4 (s, arom.), 128.3 (s, arom.), 127.7 (d, J_{CP} = 7.1 Hz, arom.), 127.6 (d, J_{CP} = 6.7 Hz, arom.), 127.2 (s, arom.), 126.5 (d, J_{CP} = 5.2 Hz, arom.), 125.7 (s, arom.), 123.9 (s, arom.), 121.3 (d, J_{CP} = 4.0 Hz, arom.), 121.0 (d, J_{CP} = 2.0 Hz, arom.), 115.2 (d, J_{CP} = 3.8 Hz, indenyl), 114.1 (br. s, indenyl), 111.3 (d, J_{CP} = 7.7 Hz, indenyl*), 110.9 (d, J_{CP} = 7.0 Hz, indenyl*), 110.7 (d, J_{CP} = 4.5 Hz, arom.), 109.9 (d, J_{CP} = 7.7 Hz, arom.), 109.7 (d, J_{CP} = 7.0 Hz, arom.), 108.4 (br. s, arom.), 91.4 (s, indenyl), 90.7 (s, indenyl*), 69.8 (d, J_{CP} = 14.3 Hz, indenyl), 68.4 (d, J_{CP} = 8.5 Hz, indenyl), 66.7 (d, J_{CP} = 5.9 Hz, indenyl*), 64.3 (d, J_{CP} = 2.6 Hz, indenyl*), 54.8 (s, NCH), 54.4 (s, NCH*), 47.2 (d, J_{CP} = 10.7 Hz, NCH_2), 47.0 (d, J_{CP} = 9.2 Hz, NCH_2*), 34.7 (d, J_{CP} = 3.8 Hz, CH_2), 34.5 (d, J_{CP} = 4.9 Hz, CH_2*), 25.4 (d, J_{CP} = 5.8 Hz, CH_2), 25.1 (d, J_{CP} = 6.0 Hz, CH_2*), 23.1 (br. s, CH_3), 22.7 (br. s, CH_3*) ppm. ^{31}P{^{1}H} NMR (121 MHz, $CDCl_3$, 25 °C): δ = 180.2 (d, $^2J_{PP}$ = 77.0 Hz, phosphoramidite), 176.8 (d, $^2J_{PP}$ = 72.8 Hz, phosphoramidite*), 61.9 (d, $^2J_{PP}$ = 77.0 Hz, PPh$_3$), 55.6 (d, $^2J_{PP}$ = 72.8 Hz, PPh$_3$*) ppm. IR (neat solid): $\tilde{\nu}$ = 3051 (w), 2964 (w), 1479 (m), 1235 (m), 1090 (m), 818 (m) cm^{-1}. HRMS: calcd. for $C_{38}H_{36}ClNO_2P_{235}{}^{102}Ru$ 737.0952; found 737.0950. $C_{38}H_{36}ClNO_2P_2Ru$ (737.17): calcd. C 61.91, H 4.92; found C 61.07, H 4.96.

[Ru(Ind)(PPh$_3$)(5a)(diphenylallenylidene)]$^+$[PF$_6$]$^-$ (15a): In a typical procedure, CH_2Cl_2 (3 mL) was added to a Schlenk flask containing complex **12b** (0.149 g, 0.145 mmol) and the orange solution was cooled to 0 °C. $(Et_3O)PF_6$ (0.036 g, 0.147 mmol) was added as a solution in CH_2Cl_2 (3 mL). The solution darkened slightly over 1 h and then 1,1-diphenyl-2-propyn-1-ol (**14a**; 0.037 g, 0.177 mmol, 1.2 equiv.) was added. The solution quickly turned dark purple. After 30 min, the cold bath was removed and the solution was warmed to room temperature over 30 min. The solvent was removed under oil-pump vacuum and the purple solid washed with Et_2O (4 × 3 mL) and dried under vacuum to give **15a** as a single diastereomer (0.163 g, 0.123 mmol, 85%); m.p. 173 °C (dec., capillary). ^{1}H NMR (300 MHz, $CDCl_3$, 25 °C): δ = 8.25 (d, $^3J_{HH}$ = 8.8 Hz, 1 H, arom.), 8.09 (d, $^3J_{HH}$ = 8.2 Hz, 1 H, arom.), 7.80 (d, $^3J_{HH}$ = 8.8 Hz, 1 H, arom.), 7.65 (d, $^3J_{HH}$ = 8.1 Hz, 1 H, arom.), 7.60–7.47 (m, 4 H, arom.), 7.34 (d, $^3J_{HH}$ = 8.5 Hz, 1 H, arom.), 7.28 (t, $^3J_{HH}$ = 7.0 Hz, 3 H, arom.), 7.22–6.70 (m, 37 H, arom.), 6.62 (d, $^3J_{HH}$ = 4.8 Hz, 2 H, arom.), 6.49 (br. s, 1 H, indenyl), 5.51 (br. s, 1 H, indenyl), 5.28 (br. s, 1 H, indenyl), 5.23 (s, CH_2Cl_2), 4.10 (d, $^2J_{HH}$ = 10.4 Hz, 1 H, NC*H*H′), 4.05 (d, $^2J_{HH}$ = 10.4 Hz, 1 H, NCH*H*′), 3.06 (d, $^2J_{HH}$ = 14.3 Hz, 1 H, NC*H*H′), 3.02 (d, $^2J_{HH}$ = 14.3 Hz, 1 H, NCH*H*′) ppm. ^{13}C{^{1}H} NMR (75 MHz, $CDCl_3$, 25 °C): δ = 293.8 (d, $^2J_{CP}$ = 21.9 Hz, C_α), 199.2 (s, C_β), 160.3 (s, C_γ), 149.4 (d, J_{CP} = 16.1 Hz, arom.), 147.9 (d, J_{CP} = 7.2 Hz, arom.), 143.0 (s, arom.), 136.6 (d, J_{CP} = 2.6 Hz, arom.), 135.0–133.0 (m, arom.), 132.6 (s, arom.), 132.5 (s, arom.), 131.8 (d, J_{CP} = 2.8 Hz, arom.), 131.5 (s, arom.), 131.4 (s, arom.), 130.9 (s, arom.), 130.1 (s, arom.), 129.4 (s, arom.), 129.3 (s, arom.), 129.2 (d, J_{CP} = 2.8 Hz, arom.), 128.9 (s, arom.), 128.8 (s, arom.), 128.7 (s, arom.), 128.6 (s, arom.), 128.5–128.1 (m, arom.), 128.0 (s, arom.), 127.7 (s, arom.), 127.1 (s, arom.), 126.9 (s, arom.), 126.4 (s, arom.), 125.8 (s, arom.), 124.6 (s, arom.), 123.4 (s, arom.), 122.5 (d, J_{CP} = 2.2 Hz, arom.), 122.1 (d, J_{CP} = 3.3 Hz, arom.), 121.6 (d, J_{CP} = 2.7 Hz, arom.), 120.2 (s, arom.), 112.3 (d, J_{CP} = 4.1 Hz, indenyl), 108.1 (s, indenyl), 94.1 (s, indenyl), 85.3 (s, indenyl), 84.2 (d, $^2J_{CP}$ =

7.0 Hz, indenyl), 50.4 (s, CH_2), 50.3 (s, CH_2') ppm. $^{31}P\{^1H\}$ NMR (121 MHz, $CDCl_3$, 25 °C): δ = 169.5 (d, $^2J_{PP}$ = 34.0 Hz, phosphoramidite), 52.3 (d, $^2J_{PP}$ = 34.0 Hz, PPh_3), –143.4 (septet, $^1J_{PF}$ = 711 Hz, PF_6) ppm. IR (neat solid): $\tilde{\nu}$ = 3056 (w), 2918 (w), 1935 (s, =C=C=C), 1586 (w), 1223 (m), 1058 (s), 1028 (s) cm^{-1}. HRMS: calcd. for $C_{76}H_{58}NO_2P_2{}^{102}Ru$ 1180.2985; found 1180.2981. $C_{76}H_{58}F_6NO_2P_3Ru\cdot(CH_2Cl_2)_{0.5}$ (1367.73): calcd. C 67.18, H 4.35; found C 67.02, H 4.55.

[Ru(Ind)(PPh_3)(5b)(methylphenylallenylidene)]$^+$[PF_6]$^-$ (15b): Yield 0.082 g (0.064 mmol, 66%) from **12b** (0.100 g, 0.0977 mmol) and **14b** (0.017 g, 0.116 mmol); m.p. 173 °C (dec., capillary). ^1H NMR (300 MHz, $CDCl_3$, 25 °C): δ = 8.30 (d, $^3J_{HH}$ = 8.7 Hz, 1 H, arom.), 8.16 (d, $^3J_{HH}$ = 8.1 Hz, 1 H, arom.), 7.87 (d, $^3J_{HH}$ = 8.4 Hz, 1 H, arom.), 7.79 (t, $^3J_{HH}$ = 7.8 Hz, 2 H, arom.), 7.72–7.54 (m, 5 H, arom.), 7.48 (d, $^3J_{HH}$ = 8.4 Hz, 1 H, arom.), 7.40–6.80 (m, 35 H, arom.), 6.56 (br. s, 1 H, indenyl), 5.38 (br. s, 2 H, indenyl), 4.01 (d, $^2J_{HH}$ = 10.8 Hz, 1 H, C*H*H′), 3.96 (d, $^2J_{HH}$ = 10.8 Hz, 1 H, CH*H*′), 3.42 (q, $^3J_{HH}$ = 7.2 Hz, 1 H, CH_2, Et_2O), 3.15 (d, $^2J_{HH}$ = 13.8 Hz, 1 H, C*H*H′), 3.10 (d, $^2J_{HH}$ = 13.8 Hz, 1 H, CH*H*′), 1.64 (s, 3 H, CH_3), 1.13 (d, $^3J_{HH}$ = 6.9 Hz, 1.5 H, CH_3, Et_2O) ppm. $^{13}C\{^1H\}$ NMR (75 MHz, $CDCl_3$, 25 °C): δ = 297.5 (dd, $^2J_{CP}$ = 23.5, $^2J_{CP}$ = 20.7 Hz, C_α), 195.5 (d, $^3J_{CP}$ = 13.8 Hz, C_β), 162.8 (s, C_γ), 149.7 (s, arom.), 149.5 (s, arom.), 147.9 (d, J_{CP} = 27.6 Hz, arom.), 141.6 (s, arom.), 136.7 (d, J_{CP} = 10.8 Hz, arom.), 134.0 (s, arom.), 133.5–133.3 (m, arom.), 132.7 (s, arom.), 131.9 (s, arom.), 131.6 (s, arom.), 131.4 (s, arom.), 131.1 (s, arom.), 130.6 (s, arom.), 129.6–127.8 (m, arom.), 127.6 (d, J_{CP} = 24.6 Hz, arom.), 127.1 (s, arom.), 126.8 (s, arom.), 126.4 (s, arom.), 125.9 (s, arom.), 124.6 (s, arom.), 123.7 (s, arom.), 122.4 (s, arom.), 121.9–121.7 (m, arom.), 120.3 (s, arom.), 112.4 (s, indenyl), 108.2 (d, $^2J_{CP}$ = 16.2 Hz, indenyl), 95.1 (s, indenyl), 83.7 (d, $^2J_{CP}$ = 30.3 Hz, indenyl), 82.7 (s, indenyl), 65.9 (s, CH_2, Et_2O), 50.3 (s, CH_2), 50.2 (s, CH_2), 30.3 (s, CH_3), 15.4 (s, CH_3, Et_2O) ppm. $^{31}P\{^1H\}$ NMR (121 MHz, $CDCl_3$, 25 °C): δ = 171.4 (d, $^2J_{PP}$ = 37.6 Hz, phosphoramidite), 53.4 (d, $^2J_{CP}$ = 37.6 Hz, PPh_3), –143.4 (septet, $^1J_{PF}$ = 711 Hz, PF_6) ppm. IR (neat solid): $\tilde{\nu}$ = 3052 (w), 1942 (s, =C=C=C), 1585 (w), 1224 (m), 1066 (w), 828 (s) cm^{-1}. HRMS: calcd. for $C_{71}H_{56}NO_2P_2{}^{102}Ru$ 1118.2828; found 1118.2827. $C_{71}H_{52}F_6NO_2P_3Ru\cdot(Et_2O)_{0.25}$ (1277.69): calcd. C 67.47, H 4.60; found C 67.28, H 4.48.

[Ru(Ind)(PPh_3)(5b){(2-furyl)methylallenylidene}]$^+$[PF_6]$^-$ (15c): Yield 0.116 g (0.0913 mmol, 94%) from **12b** (0.100 g, 0.0976 mmol) and 2-(2-furyl)-3-butyn-2-ol (**14c**; 0.014 g, 0.017 mmol); m.p. 188–190 °C (dec., capillary). ^1H NMR (300 MHz, CD_2Cl_2, 25 °C): δ = 8.23 (d, $^3J_{HH}$ = 8.8 Hz, 1 H, arom.), 8.10 (d, $^3J_{HH}$ = 8.4 Hz, 1 H, arom.), 7.89 (s, 1 H, arom.), 7.78 (d, $^3J_{HH}$ = 8.8 Hz, 1 H, arom.), 7.72–7.67 (m, 2 H, arom.), 7.57–7.51 (m, 1 H, arom.), 7.37 (d, $^3J_{HH}$ = 8.3 Hz, 1 H, arom.), 7.27–7.23 (m, 8 H, arom.), 7.17–7.12 (m, 6 H, arom.), 7.11–7.00 (m, 8 H, arom.), 7.00–6.85 (m, 13 H, arom.), 6.61–6.59 (m, 1 H, arom.), 6.37 (br. s, indenyl), 5.20 (br. s, indenyl), 5.11 (br. s, indenyl), 3.90 (d, $^2J_{HH}$ = 11.0 Hz, 1 H, C*H*H′), 3.84 (d, $^2J_{HH}$ = 11.0 Hz, 1 H, CH*H*′), 3.01 (d, $^2J_{HH}$ = 13.4 Hz, 1 H, C*H*H′), 2.95 (d, $^2J_{HH}$ = 13.4 Hz, 1 H, CH*H*′), 1.50 (s, H_2O), 1.46 (s, 3 H, CH_3) ppm. $^{13}C\{^1H\}$ NMR (75 MHz, CD_2Cl_2, 25 °C): δ = 282.7–281.6 (m, C_α), 185.2 (s, C_β), 160.9 (s, C_γ), 151.5 (s, arom.), 150.0 (d, J_{CP} = 16.1 Hz, arom.), 148.4 (d, J_{CP} = 7.3 Hz, arom.), 145.3 (s, arom.), 142.4 (s, arom.), 139.7 (s, arom.), 137.4 (br. s, arom.), 136.7 (d, J_{CP} = 10.4 Hz, arom.), 133.8 (br. s, arom.), 133.0 (s, arom.), 132.3 (s, arom.), 131.8 (s, arom.), 131.4 (d, J_{CP} = 8.4 Hz, arom.), 130.7 (br. s, arom.), 129.8 (s, arom.), 129.2 (d, J_{CP} = 4.4 Hz, arom.), 128.9 (s, arom.), 128.7 (s, arom.), 128.4 (s, arom.), 128.2 (s, arom.), 128.0 (s, arom.), 127.7 (d, J_{CP} = 4.4 Hz, arom.), 127.3 (d, J_{CP} = 6.2 Hz, arom.), 127.1 (s, arom.), 126.6 (s, arom.), 126.0 (s, arom.), 124.9 (s, arom.), 124.0 (s, arom.), 122.9 (s, arom.), 122.3–121.9 (m, arom.), 120.7 (s, arom.), 116.2 (s, arom.), 112.2 (s, indenyl), 107.6 (s, indenyl), 95.5 (s, indenyl), 82.7 (s, indenyl), 81.7 (s, indenyl), 50.4 (s, CH_2), 50.3 (s, CH_2), 28.2 (s, CH_3) ppm. $^{31}P\{^1H\}$ NMR (121 MHz, $CDCl_3$, 25 °C): δ = 174.3 (d, $^2J_{PP}$ = 38.2 Hz, phosphoramidite), 55.9 (d, $^2J_{PP}$ = 38.2 Hz, PPh_3), –143.4 (septet, $^1J_{PF}$ = 711 Hz, PF_6) ppm. IR (neat solid): $\tilde{\nu}$ = 3267 (m, H_2O), 3051 (w), 2923 (w), 1949 (s, =C=C=C), 1546 (w), 1430 (m), 1221 (m), 940 (s) cm^{-1}. HRMS: calcd. for $C_{69}H_{54}NO_3P_2{}^{102}Ru$ 1108.2622; found 1108.2654. $C_{69}H_{54}F_6NO_3P_3Ru\cdot H_2O$ (1271.17): calcd. C 65.20, H 4.44; found C 64.93, H 4.30.

[Ru(Ind)(PPh_3){(*R*)-binol-*N*,*N*-dibenzylphosphoramidite}{bis(4-fluorophenyl)allenylidene}]$^+$[PF_6]$^-$ (15d): Yield 0.135 g (0.0992 mmol, 76%) from **12b** (0.102 g, 0.0995 mmol) and 3,3-bis(4-fluorophenyl)-2-propyn-1-ol (**14d**, 0.029 g, 0.119 mmol); m.p. 196–198 °C (dec., capillary). ^1H NMR (300 MHz, $CDCl_3$, 25 °C): δ = 8.25 (d, $^3J_{HH}$ = 8.8 Hz, 1 H, arom.), 8.10 (d, $^3J_{HH}$ = 8.1 Hz, 1 H, arom.), 7.81 (d, $^3J_{HH}$ = 9.0 Hz, 1 H, arom.), 7.66 (d, $^3J_{HH}$ = 8.0 Hz, 1 H, arom.), 7.55–7.50 (m, 2 H, arom.), 7.37 (d, $^3J_{HH}$ = 8.4 Hz, 1 H, arom.), 7.26 (t, $^3J_{HH}$ = 7.6 Hz, 3 H, arom.), 7.19–7.02 (m, 16 H, arom.), 7.00–6.96 (m, 6 H, arom.), 6.95–6.90 (m, 5 H, arom.), 6.86–6.82 (m, 11 H, arom.), 6.66 (d, $^3J_{HH}$ = 8.9 Hz, 1 H, arom.), 6.56 (br. s, 1 H, indenyl), 5.53 (br. s, 1 H, indenyl), 5.22 (br. s, 1 H, indenyl), 4.07 (d, $^2J_{HH}$ = 10.5 Hz, 1 H, C*H*H′), 4.02 (d, $^2J_{HH}$ = 10.5 Hz, 1 H, CH*H*′), 3.04 (d, $^2J_{HH}$ = 14.2 Hz, 1 H, C*H*H′), 2.99 (d, $^2J_{HH}$ = 14.2 Hz, 1 H, CH*H*′) ppm. $^{13}C\{^1H\}$ NMR (75 MHz, $CDCl_3$, 25 °C): δ = 291.9–291.3 (m, C_α), 198.5 (s, C_β), 166.9 (s, C_γ), 163.5 (s, arom.), 155.5 (s, arom.), 149.3 (d, J_{CF} = 61.5 Hz, arom.), 147.8 (d, J_{CP} = 28.8 Hz, arom.), 139.2 (s, arom.), 136.6 (s, arom.), 133.7 (s, arom.), 133.6 (s, arom.), 133.2 (s, arom.), 132.4 (s, arom.), 131.7 (s, arom.), 131.3 (s, arom.), 130.8 (br. s, arom.), 130.0 (s, arom.), 129.2 (s, arom.), 128.8 (s, arom.), 128.6 (s, arom.), 128.5 (s, arom.), 128.3 (br. s, arom.), 128.0 (s, arom.), 127.6 (s, arom.), 127.1 (d, J_{CP} = 18.3 Hz, arom.), 126.9 (s, arom.), 126.4 (s, arom.), 125.9 (s, arom.), 124.8 (s, arom.), 123.5 (s, arom.), 122.4 (s, arom.), 122.0 (s, arom.), 121.6 (s, arom.), 120.0 (s, arom.), 116.4 (s, arom.), 116.1 (s, arom.), 112.4 (s, arom.), 107.6 (s, indenyl), 94.3 (s, indenyl), 85.7 (s, indenyl), 83.9 (d, $^2J_{CP}$ = 28.8 Hz, indenyl), 66.0 (s, indenyl), 50.3 (s, NCH_2), 50.1 (s, NCH_2) ppm. $^{31}P\{^1H\}$ NMR (121 MHz, $CDCl_3$, 25 °C): δ = 169.8 (d, $^2J_{PP}$ = 35.2 Hz, phosphoramidite), 52.8 (d, $^2J_{PP}$ = 35.2 Hz, PPh_3), –143.5 (septet, $^1J_{PF}$ = 711 Hz, PF_6) ppm. IR (neat solid): $\tilde{\nu}$ = 3053 (w), 1938 (s, =C=C=C), 1592 (m), 1502 (w), 1226 (m), 952 (m), 831 (s) cm^{-1}. HRMS: calcd. for $C_{76}H_{56}NO_2P_2F_2{}^{102}Ru$ 1216.2797; found 1216.2761. $C_{76}H_{56}F_8NO_2P_3Ru$ (1361.24): calcd. C 67.06, H 4.15; found C 66.60, H 3.97.

[Ru(Ind)(PPh_3)(5b){methyl(4-methoxyphenyl)allenylidene}]$^+$[PF_6]$^-$ (15e): Yield 0.083 g (0.064 mmol, 66%) from **12b** (0.100 g, 0.0979 mmol) and 2-(4-methoxylphenyl)-3-butyn-2-ol (**14e**; 0.021 g, 0.119 mmol); m.p. 150–152 °C (dec., capillary). ^1H NMR (300 MHz, $CDCl_3$, 25 °C): δ = 8.21 (d, $^3J_{HH}$ = 8.8 Hz, 1 H, arom.), 8.07 (d, $^3J_{HH}$ = 8.1 Hz, 1 H, arom.), 7.79 (d, $^3J_{HH}$ = 8.8 Hz, 1 H, arom.), 7.71–7.65 (m, 2 H, arom.), 7.53–7.49 (m, 3 H, arom.), 7.39 (d, $^3J_{HH}$ = 8.51 Hz, 1 H, arom.), 7.30–7.19 (m, 3 H, arom.), 7.18–7.10 (m, 10 H, arom.), 7.08–6.80 (m, 19 H, arom.), 6.76–6.60 (m, 4 H, arom.), 6.31 (br. s, 1 H, indenyl), 5.22 (br. s, 2 H, indenyl), 3.97 (d, $^2J_{HH}$ = 10.6 Hz, 1 H, C*H*H′), 3.92 (d, $^2J_{HH}$ = 10.6 Hz, 1 H, CH*H*′), 3.87 (s, 3 H, OCH_3), 3.02 (d, $^2J_{HH}$ = 13.0 Hz, 1 H, C*H*H′), 2.97 (d, $^2J_{HH}$ = 13.0 Hz, 1 H, CH*H*′), 1.59 (s, 3 H, CH_3) ppm. $^{13}C\{^1H\}$ NMR (75 MHz, $CDCl_3$, 25 °C): δ = 282.0 (dd, $^2J_{CP}$ = 23.5, $^2J_{CP}$ = 21.3 Hz, C_α), 181.9 (s, C_β), 166.0 (s, C_γ), 163.6 (s, arom.), 149.8 (d, J_{CP} = 15.5 Hz, arom.), 148.0 (d, J_{CP} = 7.5 Hz, arom.), 136.9 (d, J_{CP} = 2.3 Hz, arom.), 135.8 (s, arom.), 133.3 (br. s, arom.), 132.6 (s, arom.), 131.8 (s, arom.), 131.3 (s, arom.), 131.1 (s, arom.), 130.4 (br. s, arom.), 128.9 (d, J_{CP} = 2.3 Hz, arom.), 128.7

(s, arom.), 128.6 (s, arom.), 128.5 (s, arom.), 128.2 (s, arom.), 128.0 (s, arom.), 127.9 (s, arom.), 127.8 (s, arom.), 127.2 (s, arom.), 126.9 (s, arom.), 126.2 (s, arom.), 125.8 (s, arom.), 124.6 (s, arom.), 123.9 (s, arom.), 122.4 (d, J_{CP} = 2.3 Hz, arom.), 122.0 (d, J_{CP} = 3.5 Hz, arom.), 121.8 (d, J_{CP} = 2.9 Hz, arom.), 120.4 (s, arom.), 115.2 (s, arom.), 111.7 (s, arom.), 107.9 (d, $^2J_{CP}$ = 4.6 Hz, indenyl), 95.4 (s, indenyl), 81.8 (d, $^2J_{CP}$ = 7.7 Hz, indenyl), 80.2 (s, indenyl), 66.1 (s, indenyl), 56.5 (s, OCH_3), 50.1 (s, NCH_2), 50.0 (s, NCH_2'), 29.3 (s, CH_3) ppm. $^{31}P\{^1H\}$ NMR (121 MHz, $CDCl_3$, 25 °C): δ = 173.1 (d, $^2J_{PP}$ = 38.8 Hz, phosphoramidite), 54.6 (d, $^2J_{PP}$ = 38.8 Hz, PPh_3), –143.5 (septet, $^1J_{PF}$ = 711 Hz, PF_6) ppm. IR (neat solid): $\tilde{\nu}$ = 3053 (w), 1941 (s, =C=C=C), 1587 (s), 1225 (w), 1172 (m), 832 (m) cm^{-1}. HRMS: calcd. for $C_{72}H_{58}NO_3P_2{}^{102}Ru$ 1148.2935; found 1148.2966. $C_{72}H_{58}F_6NO_3P_3Ru$ (1293.22): calcd. C 66.87, H 4.52; found C 66.58, H 4.58.

X-ray Structure Determination for 5b, 12b, [15a]$^+$[PF$_6$]$^-$, [15b]$^+$[PF$_6$]$^-$, and [15d]$^+$[PF$_6$]$^-$: X-ray quality crystals of **5b** were obtained by addition of hexanes to a solution of **5b** in CH_2Cl_2 at –10 °C. X-ray quality crystals of **12b** were obtained by addition of Et_2O to a solution of **12b** in CH_2Cl_2, which was stored at –10 °C for several days. X-ray quality crystals of [**15a**]$^+$[PF_6]$^-$, [**15b**]$^+$-[PF_6]$^-$, and [**15d**]$^+$[PF_6]$^-$ were obtained by slow diffusion of Et_2O into a solution of [**15a**]$^+$[PF_6]$^-$, [**15b**]$^+$[PF_6]$^-$, and [**15d**]$^+$[PF_6]$^-$ in CH_2Cl_2 at –10 °C.

Preliminary examination and X-ray data collection were performed using a Bruker Kappa Apex II Charge-Coupled Device (CCD) Detector system single-crystal X-ray diffractometer equipped with an Oxford Cryostream LT device. Intensity data were collected by a combination of ω and ϕ scans. Apex II, SAINT, and SADABS[41] software packages were used for data collection, integration, and correction of systematic errors, respectively.

Crystal data and intensity data collection parameters are listed in Table 2. Structure solution and refinement were carried out by using the SHELXTL-PLUS software package.[39] The structures were solved by direct methods and refined successfully in the space groups *P*65 (**5b**), *P*21 (**12b**), and *P*1 ([**15a**]$^+$[PF_6]$^-$, [**15b**]$^+$[PF_6]$^-$, and [**15d**]$^+$[PF_6]$^-$). The non-hydrogen atoms were refined anisotropically to convergence. All hydrogen atoms were treated by using the appropriate riding model (AFIX m3). The structure of **12b** shows disorder in the ligand as well as in the solvent. The structure of [**15a**]$^+$[PF_6]$^-$ shows disorder in the solvent. The disorders have been modeled with partial occupancy atoms. Two phenyl rings and the six-membered ring fused to the Cp ring of [**15d**]$^+$[PF_6]$^-$ were disordered. The PF_6^- anion was also disordered. The disorders were resolved with partial occupancy atoms and were refined with geometrical restraints and thermal parameter restraints.

CCDC-798362 (for **5a**), -726745 (for **12b**), -726746 (for [**15a**][PF_6]), -730038 (for [**15b**][PF_6]), and -797367 (for [**15d**][PF_6]) contain the supplementary crystallographic data for this paper. These data can be obtained free of charge from The Cambridge Crystallographic Data Centre via www.ccdc.cam.ac.uk/data_request/cif.

Supporting Information (see footnote on the first page of this article): Experimental data for compounds **16**, dynamic NMR spectra

Table 2. Crystallographic parameters.

	5b	**12b**·(CH_2Cl_2)	[**15a**][PF_6]·(CH_2Cl_2)	[**15b**][PF_6]·(CH_2Cl_2)$_2$	[**15d**][PF_6]
Empirical formula	$C_{34}H_{26}NO_2P$	$C_{62}H_{50}Cl_3NO_2P_2Ru$	$C_{77}H_{60}Cl_2F_6NO_2P_3Ru$	$C_{73}H_{60}Cl_4F_6NO_2P_3Ru$	$C_{76}H_{56}F_8NO_2P_3Ru$
M_r	511.53	1110.39	1410.14	1433.00	1361.20
T [K]/λ [Å]	293(2)/0.71073	100(2)/0.71073	100(2)/0.71073	100(2)/0.71073	100(2)/0.71073
Crystal system	hexagonal	monoclinic	triclinic	triclinic	triclinic
Space group	*P*6(5)	$P2_1$	*P*1	*P*1	*P*1
Unit cell dimensions					
a [Å]	23.743(6)	10.6869(6)	11.2299(5)	11.0664(8)	10.7555(5)
b [Å]	23.743(6)	14.1253(8)	11.6496(5)	12.0459(10)	11.9134(5)
c [Å]	9.373(3)	17.5760(11)	14.4331(9)	13.5914(12)	14.1022(10)
α [°]	90	90	107.864(3)	107.535(4)	108.600(4)
β [°]	90	98.355(3)	99.934(2)	96.060(4)	98.130(4)
γ [°]	120	90	107.804(2)	109.111(3)	107.670(3)
V [Å^3]/Z	4576(2)/6	2625.0(3)/2	1635.53(14)/1	1589.9(2)/1	1573.99(15)/1
$\rho_{calcd.}$ [Mg m^{-3}]	1.114	1.405	1.432	1.497	1.436
Abs. coeff. [mm^{-1}]	0.118	0.558	0.461	0.557	0.399
F(000)	1608	1140	722	732	696
Crystal size [mm]	0.51 × 0.13 × 0.10	0.34 × 0.30 × 0.28	0.37 × 0.27 × 0.21	0.40 × 0.29 × 0.28	0.23 × 0.18 × 0.14
θ range [°]	2.39–25.44	1.86–4.02	2.14–35.14	1.61–33.05	1.94–27.33
Index ranges	$-28 \le h \le 28$, $-28 \le k \le 28$, $-11 \le l \le 10$	$-16 \le h \le 15$, $-15 \le k \le 22$, $-27 \le l \le 27$	$-18 \le h \le 7$, $-18 \le k \le 18$, $-23 \le l \le 23$	$-16 \le h \le 16$, $-18 \le k \le 17$, $-19 \le l \le 20$	$-13 \le h \le 13$, $-15 \le k \le 15$, $-18 \le l \le 17$
Reflections collected	95194	59037	30278	78842	57561
Independent refl.	5596 [R(int) = 0.0615]	18483 [R(int) = 0.0316]	19876 [R(int) = 0.026]	20252 [R(int) = 0.029]	13669 [R(int) = 0.055]
Abs. correction			semi-empirical from equivalents		
Max./min. transmission	0.9880/0.9420	0.8594/0.8312	0.9102/0.8464	0.8588/0.8076	0.9478/0.9132
Data/restraints/param.	5596/1/343	18483/97/715	19876/89/901	20252/23/821	13669/123/1025
Goodness-of-fit on F^2	1.090	1.020	1.018	1.046	1.070
Final R indices	R_1 = 0.0479	R_1 = 0.0485	R_1 = 0.0416	R_1 = 0.0323	R_1 = 0.0447
[$I > 2\sigma(I)$]	wR_2 = 0.1130	wR_2 = 0.1174	wR_2 = 0.1017	wR_2 = 0.0862	wR_2 = 0.1166
R indices	R_1 = 0.0873	R_1 = 0.0622	R_1 = 0.0482	R_1 = 0.0336	R_1 = 0.0494
(all data)	wR_2 = 0.1347	wR_2 = 0.1271	wR_2 = 0.1063	wR_2 = 0.0871	wR_2 = 0.1210
Largest diff. peak/hole [e Å^{-3}]	0.298/–0.233	1.984/–0.664	0.999/–0.852	1.032/–1.144	1.470/–0.859
Absolute structure parameter	–0.02(12)	–0.01(2)	–0.014(14)	–0.009(10)	–0.031(18)

for compounds **12b**, **17**, and **15a**, NMR spectra (^{1}H, ^{13}C) for all metal complexes **15** and **16**.

Acknowledgments

We thank the University of Missouri – St. Louis for support. Funding from the National Science Foundation (NSF) for the purchase of the ApexII diffractometer (MRI, CHE-0420497), the NMR spectrometer (CHE-9974801), and the mass spectrometer (CHE-9708640) is acknowledged.

[1] For reviews, see: a) V. Cadierno, J. Gimeno, *Chem. Rev.* **2009**, *109*, 3512–3560; b) C.-M. Che, C.-M. Ho, J. S. Huang, *Coord. Chem. Rev.* **2007**, *251*, 2145–2166; c) R. F. Winter, S. Záliš, *Coord. Chem. Rev.* **2004**, *248*, 1565–1583; d) S. Rigaut, D. Touchard, P. H. Dixneuf, *Coord. Chem. Rev.* **2004**, *248*, 1585–1601; e) V. Cadierno, M. P. Gamasa, J. Gimeno, *Eur. J. Inorg. Chem.* **2001**, 571–591; f) M. I. Bruce, *Chem. Rev.* **1998**, *98*, 2797–2858; g) H. Werner, *Chem. Commun.* **1997**, 903–910.

[2] a) E. O. Fischer, H.-J. Kalder, A. Frank, F. H. Köhler, G. Huttner, *Angew. Chem.* **1976**, *88*, 683; *Angew. Chem. Int. Ed. Engl.* **1976**, *15*, 623–624; b) H. Berke, *Angew. Chem.* **1976**, *88*, 684; *Angew. Chem. Int. Ed. Engl.* **1976**, *15*, 624.

[3] J. P. Selegue, *Organometallics* **1982**, *1*, 217–218.

[4] For representative examples, see: a) L.-H. Chang, C.-W. Yeh, H.-W. Ma, S.-Y. Liu, Y.-C. Lin, Y. Wang, Y.-H. Liu, *Organometallics* **2010**, *29*, 1092–1099; b) L. T. Byrne, G. A. Koutsantonis, V. Sanford, J. P. Selegue, P. A. Schauer, R. S. Iyer, *Organometallics* **2010**, *29*, 1199–1209; c) A. García-Fernández, M. P. Gamasa, E. Lastra, *J. Organomet. Chem.* **2010**, *695*, 162–169; d) J. A. Pino-Chamorro, E. Bustelo, M. C. Puerta, P. Valerga, *Organometallics* **2009**, *28*, 1546–1557; e) E. A. Shaffer, C. L. Chen, A. M. Beatty, E. J. Valente, H.-J. Schanz, *J. Organomet. Chem.* **2007**, *692*, 5221–5233; f) S. Conejero, J. Díez, M. P. Gamasa, J. Gimeno, *Organometallics* **2004**, *23*, 6299–6310; g) V. Cadierno, S. Conejero, M. P. Gamasa, J. Gimeno, M. A. Rodríguez, *Organometallics* **2002**, *21*, 203–209; h) V. Cadierno, S. Conejero, M. P. Gamasa, J. Gimeno, L. R. Falvello, R. M. Llusar, *Organometallics* **2002**, *21*, 3716–3726; i) R. F. Winter, K.-W. Klinkhammer, *Organometallics* **2001**, *20*, 1317–1333; j) A. Fürstner, M. Liebl, C. W. Lehmann, M. Picquet, R. Kunz, C. Bruneau, D. Touchard, P. H. Dixneuf, *Chem. Eur. J.* **2000**, *6*, 1847–1857; k) V. Cadierno, M. P. Gamasa, J. Gimeno, M. González-Cueva, E. Lastra, J. Borge, S. García-Granda, E. Pérez-Carreño, *Organometallics* **1996**, *15*, 2137–2147; l) M. A. Esteruelas, A. V. Gómez, F. J. Lahoz, A. M. López, E. Oñate, L. A. Oro, *Organometallics* **1996**, *15*, 3423–3435; m) R. F. Winter, *Eur. J. Inorg. Chem.* **1999**, 2121–2126.

[5] a) N. Szesni, M. Drexler, J. Maurer, R. F. Winter, F. de Montigny, C. Lapinte, S. Steffens, J. Heck, B. Weibert, H. Fischer, *Organometallics* **2006**, *25*, 5774–5787; b) W.-S. Ojo, F. Y. Pétillon, P. Schollhammer, J. Talarmin, K. W. Muir, *Organometallics* **2006**, *25*, 5503–5505; c) C. Bianchini, N. Mantovani, L. Marvelli, M. Peruzzini, R. Rossi, A. Romerosa, *J. Organomet. Chem.* **2001**, *617–618*, 233–241; d) K. Ilg, H. Werner, *Organometallics* **2001**, *20*, 3782–3794; e) C. Gauss, D. Veghini, O. Orama, H. Berke, *J. Organomet. Chem.* **1997**, *541*, 19–38; f) R. Castarlenas, M. A. Esteruelas, R. Lalrempuia, M. Oliván, E. Oñate, *Organometallics* **2008**, *27*, 795–798; g) A. Collado, M. A. Esteruelas, F. López, J. L. Mascareñas, E. Oñate, B. Trillo, *Organometallics*, DOI: 10.1021/om100192t; h) F. Kessler, N. Szesni, K. Põhako, B. Weibert, H. Fischer, *Organometallics* **2009**, *28*, 348–354; i) F. Kessler, B. Weibert, H. Fischer, *Organometallics*, DOI: 10.1021/om100346x.

[6] M. Hussain, S. Kohser, K. Janssen, R. Wartchow, H. Butenschön, *Organometallics* **2009**, *28*, 5212–5221.

[7] a) C. Bruneau, P. H. Dixneuf, *Angew. Chem.* **2006**, *118*, 2232; *Angew. Chem. Int. Ed.* **2006**, *45*, 2176–2203; b) I. Dragutan, V. Dragutan, *Platinum Met. Rev.* **2006**, *50*, 81–94; c) B. M. Trost, M. U. Frederiksen, M. T. Rudd, *Angew. Chem.* **2005**, *117*, 6788; *Angew. Chem. Int. Ed.* **2005**, *44*, 6630–6666.

[8] a) A. Fürstner, M. Picquet, C. Bruneau, P. H. Dixneuf, *Chem. Commun.* **1998**, 1315–1316; b) A. Fürstner, A. F. Hill, M. Liebl, J. D. E. T. Wilton-Ely, *Chem. Commun.* **1999**, 601–602; c) R. Castarlenas, C. Vovard, C. Fischmeister, P. H. Dixneuf, *J. Am. Chem. Soc.* **2006**, *128*, 4079–4089; d) C. E. Diesendruck, E. Tzur, N. G. Lemcoff, *Eur. J. Inorg. Chem.* **2009**, 4185–4203; e) X. Sauvage, Y. Borguet, G. Zaragoza, A. Demonceau, *Adv. Synth. Catal.* **2009**, *351*, 441–455; f) N. Ledoux, R. Drozdzak, B. Allaert, A. Linden, P. Van Der Voort, F. Verpoort, *Dalton Trans.* **2007**, 5201–5210.

[9] S. M. Maddock, M. G. Finn, *Angew. Chem.* **2001**, *113*, 2196; *Angew. Chem. Int. Ed.* **2001**, *40*, 2138–2141.

[10] N. Auger, D. Touchard, S. Rigaut, J.-F. Halet, J.-Y. Saillard, *Organometallics* **2003**, *22*, 1638–1644.

[11] a) T. Bolaño, R. Castarlenas, M. A. Esteruelas, E. Oñate, *Organometallics* **2008**, *27*, 6367–6370; b) E. Bustelo, M. Jiménez-Tenorio, K. Mereiter, M. C. Puerta, P. Valerga, *Organometallics* **2002**, *21*, 1903–1911; c) M. I. Bruce, P. J. Low, E. R. T. Tiekink, *J. Organomet. Chem.* **1999**, *572*, 3–10; d) D. J. Bernad, M. A. Esteruelas, A. M. López, J. Modrego, M. C. Puerta, P. Valerga, *Organometallics* **1999**, *18*, 4995–5003.

[12] V. Cadierno, M. P. Gamasa, J. Gimeno, E. Pérez-Carreño, S. García-Granda, *Organometallics* **1999**, *18*, 2821–2832.

[13] K. M. Nicholas, *Acc. Chem. Res.* **1987**, *20*, 207–214.

[14] a) Y. Tanabe, K. Kanao, Y. Miyake, Y. Nishibayashi, *Organometallics* **2009**, *28*, 1138–1142; b) Y. Yamauchi, Y. Miyake, Y. Nishibayashi, *Organometallics* **2009**, *28*, 48–50; c) M. Daini, M. Yoshikawa, Y. Inada, S. Uemura, K. Sakata, K. Kanao, Y. Miyake, Y. Nishibayashi, *Organometallics* **2008**, *27*, 2046–2051; d) Y. Yada, Y. Miyake, Y. Nishibayashi, *Organometallics* **2008**, *27*, 3614–3617; e) Y. Nishibayashi, S. Uemura, *Curr. Org. Chem.* **2006**, *10*, 135–150.

[15] V. Cadierno, J. Díez, S. E. García-Garrido, J. Gimeno, *Chem. Commun.* **2004**, 2716–2717.

[16] a) K. Kanao, Y. Miyake, Y. Nishibayashi, *Organometallics* **2010**, *29*, 2126–2131; b) K. Kanao, Y. Miyake, Y. Nishibayashi, *Organometallics* **2009**, *28*, 2920–2926; c) K. Fukamizu, Y. Miyake, Y. Nishibayashi, *J. Am. Chem. Soc.* **2008**, *130*, 10498–10499; d) H. Matsuzawa, K. Kanao, Y. Miyake, Y. Nishibayashi, *Org. Lett.* **2007**, *9*, 5561–5564; e) H. Matsuzawa, Y. Miyake, Y. Nishibayashi, *Angew. Chem.* **2007**, *119*, 6608; *Angew. Chem. Int. Ed.* **2007**, *46*, 6488–6491; f) Y. Inada, Y. Nishibayashi, S. Uemura, *Angew. Chem.* **2005**, *117*, 7893; *Angew. Chem. Int. Ed.* **2005**, *44*, 7715–7717.

[17] a) Y. Nishibayashi, H. Imajima, G. Onodera, S. Uemura, *Organometallics* **2005**, *24*, 4106–4109; b) V. Cadierno, S. Conejero, M. P. Gamasa, J. Gimeno, *Organometallics* **2001**, *20*, 3175–3189; c) V. Cadierno, S. Conejero, M. P. Gamasa, J. Gimeno, *Dalton Trans.* **2003**, 3060–3066; d) K. Kanao, Y. Tanabe, Y. Miyake, Y. Nishibayashi, *Organometallics* **2010**, *29*, 2381–2384.

[18] a) A. García-Fernández, J. Gimeno, E. Lastra, C. A. Madrigal, C. Graiff, A. Tiripicchio, *Eur. J. Inorg. Chem.* **2007**, 732–741; b) Y.-W. Zhong, Y. Matsuo, E. Nakamura, *Chem. Asian J.* **2007**, *2*, 358–366.

[19] a) C. Ganter, *Chem. Soc. Rev.* **2003**, *32*, 130–138; b) J. W. Faller, J. Parr, A. R. Lavoie, *New J. Chem.* **2003**, *27*, 899–901; c) H. Brunner, *Eur. J. Inorg. Chem.* **2001**, 905–912.

[20] For representative examples, see: a) D. Carmona, M. P. Lamata, F. Viguri, R. Rodríguez, F. J. Lahoz, M. J. Fabra, L. A. Oro, *Tetrahedron: Asymmetry* **2009**, *20*, 1197–1205; b) S. J. Malcolmson, S. J. Meek, E. S. Sattely, R. R. Schrock, A. H. Hoveyda, *Nature* **2008**, *456*, 933–937; c) O. Hamelin, M. Rimboud, J. Pécaut, M. Fontecave, *Inorg. Chem.* **2007**, *46*, 5354–5360; d) M. Lasa, P. López, C. Cativiela, C. Carmona, L. A. Oro, *J. Mol. Catal. A* **2005**, *234*, 129–135; e) K. Kromm, P. L. Osburn, J. A. Gladysz, *Organometallics* **2002**, *21*, 4275–4280; f)

J. W. Faller, B. J. Grimmond, *Organometallics* **2001**, *20*, 2454–2458.
[21] a) J. F. Teichert, B. L. Feringa, *Angew. Chem.* **2010**, *122*, 2538; *Angew. Chem. Int. Ed.* **2010**, *49*, 2486–2528; b) R. Hulst, N. K. de Vries, B. L. Feringa, *Tetrahedron: Asymmetry* **1994**, *5*, 699–708; c) B. L. Feringa, *Acc. Chem. Res.* **2000**, *33*, 346–353; d) A. Duursma, J.-G. Boiteau, L. Lefort, J. A. F. Boogers, A. H. M. de Vries, J. G. de Vries, A. J. Minnaard, B. L. Feringa, *J. Org. Chem.* **2004**, *69*, 8045–8052; e) R. Hoen, M. van den Berg, H. Bernsmann, A. J. Minnaard, J. G. de Vries, B. L. Feringa, *Org. Lett.* **2004**, *6*, 1433–1436; f) I. S. Mikhel, H. Rüegger, P. Butti, F. Camponovo, D. Huber, A. Mezzetti, *Organometallics* **2008**, *27*, 2937–2948; g) T. Osswald, I. S. Mikhel, H. Rüegger, P. Butti, A. Mezzetti, *Inorg. Chim. Acta* **2010**, *363*, 474–480; h) T. Osswald, H. Rüegger, A. Mezzetti, *Chem. Eur. J.* **2010**, *16*, 1388–1397.
[22] For recent examples, see: a) S. M. Smith, J. M. Takacs, *Org. Lett.* **2010**, *12*, 4612–4615; b) M. Roggen, E. M. Carreira, *J. Am. Chem. Soc.* **2010**, *132*, 11917–11919; c) M. A. Fernández-Zúmel, B. Lastra-Barreira, M. Scheele, J. Díez, P. Crochet, J. Gimeno, *Dalton Trans.* **2010**, *39*, 7780–7785; d) X.-C. Qiao, S.-F. Zhu, W.-Q. Chen, Q.-L. Zhou, *Tetrahedron: Asymmetry* **2010**, *21*, 1216–1220; e) N. Mršić, T. Jerphagnon, A. J. Minnaard, B. L. Feringa, J. G. de Vries, *Tetrahedron: Asymmetry* **2010**, *21*, 7–10; f) L. M. Stanley, C. Bai, M. Ueda, J. F. Hartwig, *J. Am. Chem. Soc.* **2010**, *132*, 8918–8920; g) J. A. Raskatov, S. Spiess, C. Gnamm, K. Brödner, F. Rominger, G. Helmchen, *Chem. Eur. J.* **2010**, *16*, 6601–6615; h) A. Mercier, X. Urbaneja, W. C. Yeo, P. D. Chaudhuri, G. R. Cumming, D. House, G. Bernardinelli, E. P. Kündig, *Chem. Eur. J.* **2010**, *16*, 6285–6299; i) L. Palais, L. Babel, A. Quintard, S. Belot, A. Alexakis, *Org. Lett.* **2010**, *12*, 1988–1991; j) H. He, W.-B. Liu, L.-X. Dai, S.-L. You, *Angew. Chem.* **2010**, *122*, 1538; *Angew. Chem. Int. Ed.* **2010**, *49*, 1496–1499; k) J.-L. Zeng, S.-B. Yu, Z. Cao, D.-W. Yang, *Catal. Lett.* **2010**, *136*, 243–248; l) M. Batuecas, M. A. Esteruelas, C. García-Yebra, E. Oñate, *Organometallics* **2010**, *29*, 2166–2175.
[23] S. Costin, N. P. Rath, E. B. Bauer, *Inorg. Chim. Acta* **2009**, *362*, 1935–1942.
[24] M. E. Rerek, L.-N. Ji, F. Basolo, *J. Chem. Soc., Chem. Commun.* **1983**, 1208–1209.
[25] a) X. Xu, Y. Chen, J. Feng, G. Zou, J. Sun, *Organometallics* **2010**, *29*, 549–553; b) M. Lenze, S. L. Sedinkin, N. P. Rath, E. B. Bauer, *Tetrahedron Lett.* **2010**, *51*, 2855–2858; c) C. E. Garrett, G. C. Fu, *J. Org. Chem.* **1998**, *63*, 1370–1371.
[26] a) J. M. O'Connor, C. P. Casey, *Chem. Rev.* **1987**, *87*, 307–318; b) M. P. Gamasa, J. Gimeno, C. Gonzalez-Bernardo, B. M. Martín-Vaca, *Organometallics* **1996**, *15*, 302–308; c) V. Cadierno, J. Diez, M. P. Gamasa, J. Gimeno, E. Lastra, *Coord. Chem. Rev.* **1999**, *193–195*, 147–205; d) M. J. Calhorda, C. C. Romão, L. F. Veiros, *Chem. Eur. J.* **2002**, *8*, 868–875; e) E. J. Derrah, J. C. Marlinga, D. Mitra, D. M. Friesen, S. A. Hall, R. McDonald, L. Rosenberg, *Organometallics* **2005**, *24*, 5817–5827.
[27] S. Costin, N. P. Rath, E. B. Bauer, *Tetrahedron Lett.* **2009**, *50*, 5485–5488.
[28] L. A. Oro, M. A. Ciriano, M. Campo, *J. Organomet. Chem.* **1985**, *289*, 117–131.
[29] M. Hölscher, G. Franció, W. Leitner, *Organometallics* **2004**, *23*, 5606–5617.
[30] J. P. Selegue, B. A. Young, S. L. Logan, *Organometallics* **1991**, *10*, 1972–1980.
[31] a) A. Antonucci, M. Bassetti, C. Bruneau, P. H. Dixneuf, C. Pasquini, *Organometallics* **2010**, *29*, 4524–4531; b) H.-J. Schanz, L. Jafarpour, E. D. Stevens, S. P. Nolan, *Organometallics* **1999**, *18*, 5187–5190.
[32] H. Kopf, C. Pietraszuk, E. Hübner, N. Burzlaff, *Organometallics* **2006**, *25*, 2533–2546.
[33] C. R. Smith, D. J. Mans, T. V. RajanBabu, *Org. Synth.* **2008**, *85*, 238–247.
[34] F. M. Semmelhack, N. Jeong, *Tetrahedron Lett.* **1990**, *31*, 605–608.
[35] a) C. Botteghi, M. Marchetti, S. Paganellia, F. Persi-Paoli, *Tetrahedron* **2001**, *57*, 1631–1637; b) J. S. Schneekloth Jr., M. Pucheault, C. M. Crews, *Eur. J. Org. Chem.* **2007**, 40–43.
[36] The asterisk (*) denotes the second (minor) diastereomer.
[37] Peaks corresponding to the minor diastereomer were not observed.
[38] The methine proton is not visible and is assumed to be overlapped by aromatic protons.
[39] G. M. Sheldrick, *Acta Crystallogr., Sect. A* **2008**, *64*, 112–122.
[40] C. F. Macrae, I. J. Bruno, J. A. Chisholm, P. R. Edgington, P. McCabe, E. Pidcock, L. Rodriguez-Monge, R. Taylor, J. van de Streek, P. A. Wood, *J. Appl. Crystallogr.* **2008**, *41*, 466–470.
[41] Bruker Analytical X-ray, Madison, WI, **2008**; Bruker Analytical X-ray, Madison, WI, **2010**.

Received: November 4, 2010
Published Online: February 2, 2011

